LBNL-50991
Preprint

CO_2-H_2O Mixtures in the Geological Sequestration of CO_2. I. Assessment and Calculation of Mutual Solubilities from 12 to 100 °C and up to 600 bar.

Nicolas Spycher, Karsten Pruess

Earth Sciences Division

and

Jonathan Ennis-King

CSIRO Petroleum

July 2002

Submitted to
Geochimica et Cosmochimica Acta

LBNL-50991

CO_2-H_2O MIXTURES IN THE GEOLOGICAL SEQUESTRATION OF CO_2. I. ASSESSMENT AND CALCULATION OF MUTUAL SOLUBILITIES FROM 12 TO 100 °C AND UP TO 600 BAR.

NICOLAS SPYCHER

KARSTEN PRUESS

Earth Sciences Division, Lawrence Berkeley National Laboratory
MS 90-1116, 1 Cyclotron Road, Berkeley, California, USA

and

JONATHAN ENNIS-KING

CSIRO Petroleum, P.O. Box 3000, Glen Waverley 3150, Australia

Submitted to *Geochimica et Cosmochimica Acta*

July 2002

This work was supported by the US Department of Energy through the Office of Basic Energy Sciences under Contract No. DE-AC03-76SF00098. One author (JEK) wishes to acknowledge support from the Australian Petroleum Cooperative Research Center's GEODISC project.

CO_2-H_2O Mixtures in the Geological Sequestration of CO_2. I. Assessment and Calculation of Mutual Solubilities from 12 to 100 °C and up to 600 bar.

Nicolas Spycher[1], Karsten Pruess[1], and Jonathan Ennis-King[2]
[1]Lawrence Berkeley National Laboratory, MS 90-1116, 1 Cyclotron Road, Berkeley, California, USA
[2]CSIRO Petroleum, P.O. Box 3000, Glen Waverley 3150, Australia

July 2002

Abstract

Evaluating the feasibility of CO_2 geologic sequestration requires the use of pressure-temperature-composition (P-T-X) data for mixtures of CO_2 and H_2O at moderate pressures and temperatures (typically below 500 bar and below 100°C). For this purpose, published experimental P-T-X data in this temperature and pressure range are reviewed. These data cover the two-phase region where a CO_2-rich phase (generally gas) and an H_2O-rich liquid coexist and are reported as the mutual solubilities of H_2O and CO_2 in the two coexisting phases. For the most part, mutual solubilities reported from various sources are in good agreement. The mixing behavior of H_2O in the compressed gas phase is highly nonideal. A noniterative procedure is presented to calculate the composition of the compressed CO_2 and liquid H_2O phases at equilibrium, based on equating chemical potentials and using the Redlich-Kwong equation of state to express departure from ideal behavior. The procedure is an extension of that used by King et al. (1992), covering a broader range of temperatures and experimental data than those authors, and is readily expandable to a nonideal liquid phase. The calculation method and formulation are kept as simple as possible to avoid degrading the performance of numerical models of water-CO_2 flows for which they are intended. The method is implemented in a computer routine, and inverse modeling is used to determine, simultaneously, new Redlich-Kwong parameters for the H_2O-CO_2 mixture, as well as aqueous solubility constants for gaseous and liquid CO_2 as a function of temperature. In doing so, mutual solubilities of H_2O from 12 to 100°C and CO_2 from 15 to 110°C and up to 600 bar are generally reproduced within a few percent of experimental values. Fugacity coefficients of pure CO_2 are reproduced mostly within one percent of published reference data.

Introduction

The potential for global warming caused by the production of carbon dioxide from burning fossil fuels is generating an increasing interest in the study of carbon dioxide sequestration (e.g., DOE, 1999). One sequestration method currently attracting attention from the scientific community consists of injecting carbon dioxide into saline aquifers (e.g., Pruess and Garcia, 2002), abandoned hydrocarbon reservoirs, or unminable coal seams. Predicting the sequestration potential and long-term behavior of man-made geologic reservoirs requires calculating the pressure, temperature, and composition (P-T-X) properties of CO_2-H_2O mixtures at depths where temperatures remain below 100°C but where pressures may reach several hundred bar. In this P-T range, two phases typically coexist: a CO_2-rich gas or liquid phase and an H_2O-rich liquid phase. At temperatures below 100°C, the amount of H_2O in the CO_2-rich phase is quite small, such that the CO_2 properties can be approximated fairly well by those of pure CO_2. However, H_2O in the CO_2-rich phase exhibits a strong nonideal mixing behavior (e.g., King et al., 1992; Spycher and Reed, 1988). The first task in this study was, therefore, to review existing experimental data on the mutual solubilities of CO_2 and H_2O at temperatures below 100°C and pressures up to 600 bar. The initial focus was more on the H_2O solubility in CO_2 than the solubility of CO_2 in water, because the latter has been the subject of more published investigations. The next step was to implement calculation methods suitable to reproduce the experimental data with sufficient accuracy for the study of geologic CO_2 disposal, but enough simplicity to avoid degrading the performance of numerical models for which these methods are intended. The present study considers only the two-component system H_2O-CO_2. Because dissolved solids would affect the phase partitioning of H_2O and CO_2, further studies are underway to consider the impact of dissolved salts on the mutual solubilities of H_2O and CO_2.

Phase Properties in the P-T Range of CO_2 Geological Sequestration

The complete phase diagram of CO_2-H_2O systems has been discussed by numerous authors (Todheide and Frank,1963; Takenouchi and Kennedy, 1964; Evelein et al.,1976). However, in this study, only the low-temperature behavior is of interest for applications to geological CO_2 storage. Figure 1 shows the location of all the literature data used in

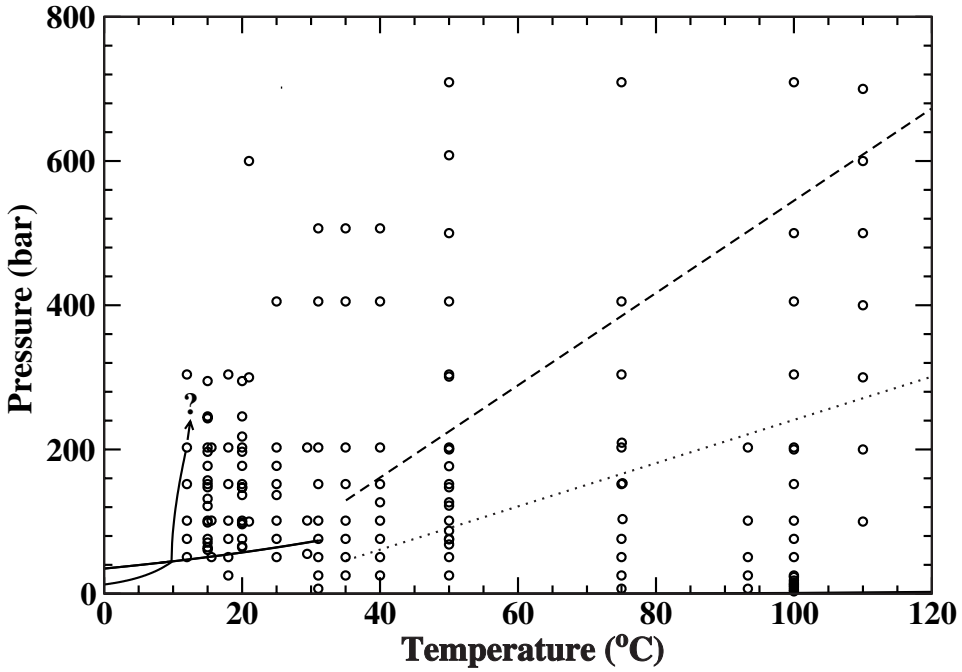

Figure 1. P-T cross section of the CO_2-H_2O phase diagram, showing the location of all the literature data points used in this study (open circles) and indicating typical subsurface conditions for geological storage. The lower dotted line gives typical equilibrium subsurface conditions for CO_2 storage (see text). The upper dotted line gives typical maximum injection pressure conditions, assuming thermal equilibrium (see text). The solid lines are phase coexistence curves as detailed in Figure 2. The question mark indicates uncertainty about the location of the hydrate formation curve at high pressures.

this study on a projection of the CO_2-H_2O phase diagram on a P-T plane. The solid lines are the two- and three-phase coexistence curves explained further below and detailed in Figure 2. The lower dotted line indicates typical equilibrium subsurface conditions, based on a mean surface temperature of 20°C, a geothermal gradient of 35°C/km and a hydrostatic pressure gradient of 105 bar/km. The upper dotted curve indicates typical maximum injection pressures, using a mean surface temperature of 15°C, a geothermal gradient of 25°C/km, and a maximum injection pressure gradient of 160 bar/km (based on 90% of a typical fracture pressure gradient). This last curve assumes that the injected CO_2 is at the same temperature as the formation, which should be valid away from the well. Near the well, a lower temperature would be expected. The starting depth of interest is 800 m, which corresponds to a temperature of 35°C using a mean surface temperature of 15°C and a geothermal gradient of 25°C/km.

There is a higher density of data in the subcritical temperature range most easily accessible to experimenters (Figure 1), whereas only about 12% of the data falls in the P-T range of most interest for geological storage. Nevertheless the data outside this range is useful for fitting and validating the representation used here, and it may also be valuable in analyzing possible scenarios in which CO_2 might migrate to shallower depths. The question mark in Figure 1 indicates uncertainty about the location of the hydrate formation curve at high pressures, and this may cast some doubt on the validity of low temperature solubility measurements in that region.

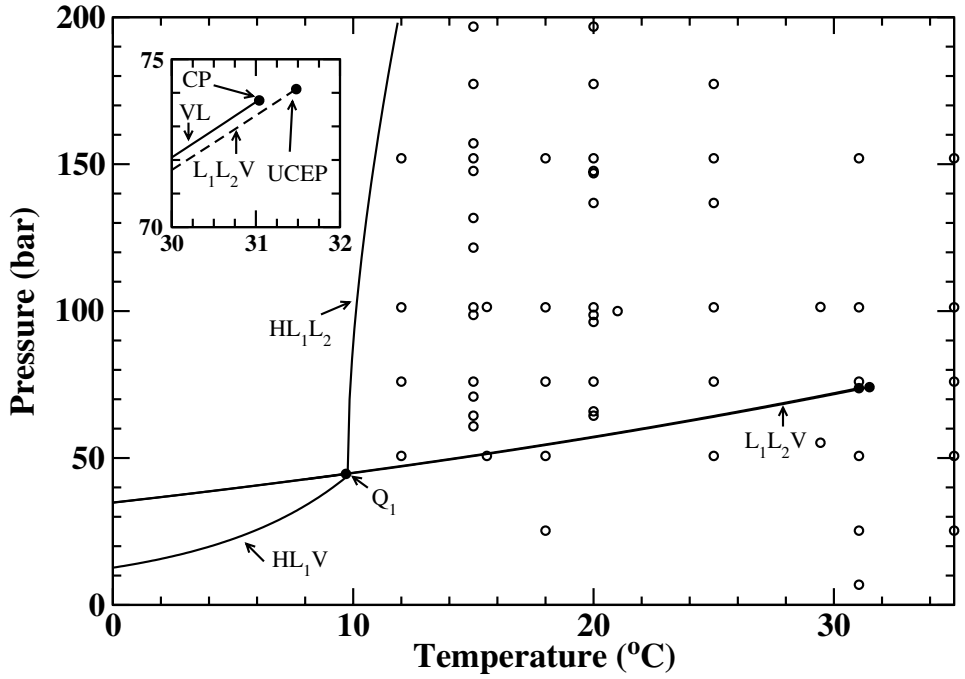

Figure 2. Enlarged P-T cross section of the CO_2-H_2O phase diagram, showing the two- and three-phase coexistence curves and the critical points. The circles are literature data points used in this study. The dashed curves are three-phase coexistence curves as labeled (vapor phase V, water-rich liquid L_1, CO_2-rich liquid L_2, and hydrate phase H). The solid curve is the liquid-vapor coexistence curve for pure CO_2 (VL). The inset shows that this pure-CO_2 liquid-vapor curve almost coincides with the three-phase coexistence curve for the H_2O-CO_2 system (L_1L_2V). CP is the critical point of pure carbon dioxide, UCEP is the upper critical end-point for the CO_2-H_2O system, and Q_1 is a quadruple point for that system.

Figure 2 gives a more detailed view of the two- and three-phase coexistence curves at low temperatures. The solid line is the vapor-liquid (VL) coexistence curve for pure CO_2 (representation from Angus et al., 1976), while the dashed lines are the various three-

phase coexistence curves for the H_2O-CO_2 system (H stands for the hydrate phase, L_1 for a water-rich liquid and L_2 for a CO_2 rich liquid). The L_1L_2V and HL_1V curves are based on the representations given by Wendland et al. (1999). The HL_1L_2 curve has been fitted to literature data (Ng and Robinson, 1985; Fan and Guo, 1999), using the functional form $P/P_q = 1+ 32.33\ (T/T_q -1)^{1/2} + 91.169\ (T/T_q-1)$ where T_q=9.77°C and P_q=44.60 bar are the location of the quadruple point Q_1 at which all four phases coexist. Because the data of Ng and Robinson (1985) for the hydrate formation curve HL_1L_2 only goes up to 140 bar, this representation is not reliable for extrapolation to pressures much above this value. The inset in Figure 2 shows that the VL curve and the L_1L_2V curve almost coincide, so that the CO_2 critical point (31.06°C and 73.825 bar from Angus, 1973, or 30.978 +/- 0.015°C and 73.773 +/- 0.03 bar from Span and Wagner, 1996) is very close to the upper critical end point (31.48°C and 74.11 bar, Wendland et al.,1999). Most of the literature data shown fall either in the L_1L_2 regime, in which a water-rich liquid phase coexists with a CO_2-rich liquid, or in the regime above the critical temperature and/or pressure of CO_2, where the distinction between the vapor and liquid phases of CO_2 disappears.

The narrow three-phase coexistence pressure interval in the CO_2-H_2O system is further illustrated on Figure 3, which shows a P-X cross section of the CO_2-H_2O phase diagram at 25°C (i.e., a section perpendicular to the plan of Figure 2 at 25°C). The inset of this figure is shown using approximate pressure values. Wenland et al. (1999) report a three-phase coexistence pressure of 64.03 bar at 298.16K. The pure CO_2 vapor pressure extrapolated at the same temperature from the data of Angus et al. (1976) is 64.31 bar. The main consequence of this narrow three-phase coexistence pressure interval for the data analysis is that isotherms that cross the L_1L_2V coexistence curve (below 31°C) exhibit a sharp discontinuity in the solubility of H_2O in the CO_2 phase (Figure 3), but otherwise the data are continuous. Owing to its narrowness and its location in P-T space, the three-phase region is of little importance for geological sequestration, except perhaps for escaping CO_2 which might be at lower pressures and temperatures, and for parts of the CO_2 injection system.

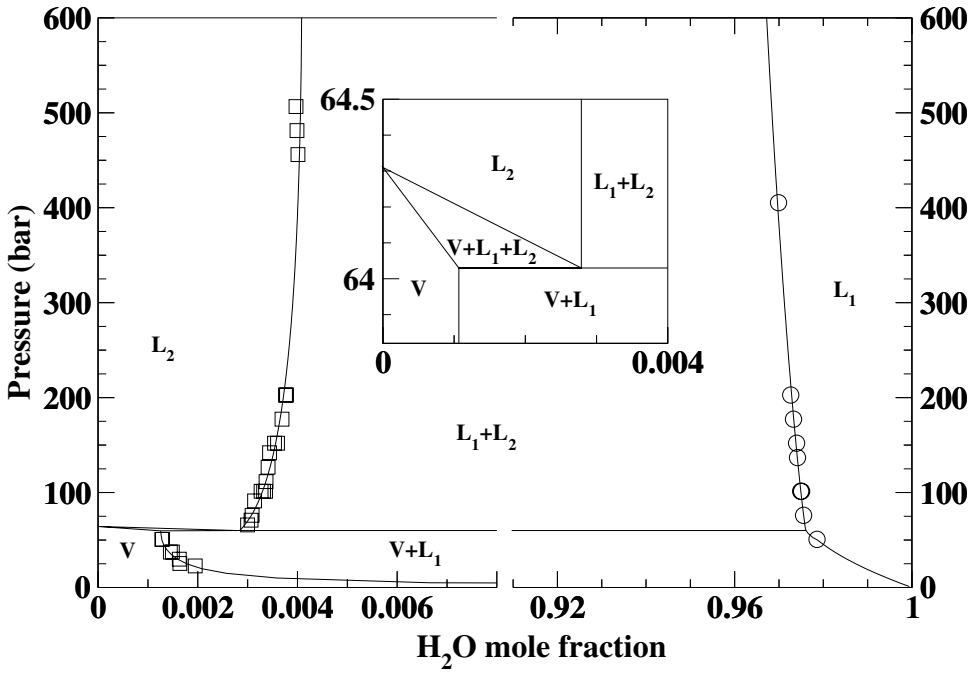

Figure 3. Pressure-mole fraction cross section of the CO_2-H_2O phase diagram at 25°C. Circles are literature data points for CO_2 solubility in H_2O; squares are for H_2O solubility in CO_2. Solid curves are drawn to delimit the various phase coexistence regions: V is the vapor phase, L_1 is the H_2O-rich liquid phase and L_2 is the CO_2-rich liquid phase. The inset shows the three-phase coexistence region in greater detail. See text. Note the difference in the horizontal scale between the two parts of the graph.

Review of Experimental Solubility Data

Most of the early experimental work on H_2O-CO_2 mixtures focused on high temperatures and pressures applicable to the study of metamorphic processes (typically several hundred degrees C and up to several kilobar) (e.g., Mäder, 1991). Published data in the two-phase region at temperatures below 100°C and at moderate pressures were initially more limited. However, in the last two decades, more data have become available in this P-T range. Early studies include those by Wiebe and Gaddy (1939, 1940, and 1941), Todheide and Frank (1963), and Coan and King (1971). More recent work on the two-phase region below 100°C was performed by Gillepsie and Wilson (1982), Briones et al. (1987), Song and Kobayashi (1987), D'Souza et al. (1988), Müller et al. (1988), and Sako et al. (1991), King et al. (1992) and Dohrn et al. (1993). Recent experimental studies providing additional data on the solubility of CO_2 in water (but no information on coexisting gas-phase compositions) within our P-T range of interest include those of Teng et al. (1997), Jackson et al. (1995) and Rosenbauer et al. (2001). Data from all

these sources are summarized in Appendix A and tabulated by temperature. Only data points down to 12ºC and up to 110ºC are listed in Appendix A. Teng et al. (1997) reports data at lower temperatures, which we do not consider because of the potential for clathrate formation below 12ºC (Figure 2) (see also Anderson 2002; Wiebe and Gaddy 1940). Data at 110°C from the work of Takenouchi and Kennedy (1964) are included in Appendix A and used in discussions near the end of this paper. Data points above 110ºC from these authors and from Müller et al. (1988) are not listed or considered further because they are outside our targeted temperature range.

A number of other experimental studies on CO_2 solubility in water have been conducted besides those listed above. These studies cover pressures mostly below 50 bar and temperatures outside our range of interest, or they do not include data on the composition of the coexisting CO_2-rich phase. For these reasons, data from these studies were not considered. Most of these studies were reviewed by Crovetto (1991) and Carroll and Mather (1992) to derive Henry's law constants for CO_2 in water. As discussed later, solubilities calculated from the data in Appendix A, using algorithms developed in this study, generally agree well with those calculated by these authors.

The mutual solubilities of H_2O and CO_2 from 12 to 110°C and up to 600 bar (in Appendix A) are shown as symbols on Figures 4, 5, and 6. Data on these figures correspond to the branches of the P-X phase diagram shown with superposed symbols on Figure 3. Curves show solubilities calculated using methods discussed later. Overlapping data sets are in fairly good agreement, as discussed below.

H_2O Solubility in the CO_2-Rich Phase

The H_2O solubilities reported by Coan and King (1971) at 25, 50, and 75°C and by King et al. (1992) at 25°C generally agree with those of Wiebe and Gaddy (1940) within a few percent. Solubilities reported by Gillepsie and Wilson (1982), Briones et al. (1987) and Song and Kobayashi (1987) generally fall in line with these data. At 50°C, the H_2O solubility measured by D'Souza et al. (1988) at 152 bar falls noticeably (25% or so) above the trend defined by the other data (Figure 5). The H_2O solubilities reported by

Dohrn et al. (1993) at 50°C fall somewhat above the other solubility values near 100 and 300 bar, but agree closely with the data of Wiebe and Gaddy (1941) near 200 bar (Figure 5). The two high-pressure data points (near 345 bar) from Jackson et al. (1995) at 50 and 75°C fall near the trend defined by Wiebe and Gaddy's data, with better agreement at 50 than at 75°C (Figure 6). At 75°C above 100 bar, the H_2O solubilities measured by Gillepsie and Wilson (1987), D'Souza et al. (1988), and Sako et al. (1991) fall noticeably below the trend of solubilities defined by the data of Wiebe and Gaddy (1941) and Jackson et al. (1995) (up to 25% lower for data of Sako et al.,1991) (Figure 6). One point of Wiebe and Gaddy (1941) at 75°C and 25 bar also plots significantly off-trend, as already noticed by Coan and King (1971) (Figure 6). Greenwood and Barnes (1966) report H_2O solubilities at 100°C and cite Wiebe and Gaddy (1939, 1940, 1941) as references. However, Wiebe and Gaddy do not report gas-phase compositions above 75°C, and presumably these data were extrapolated from Wiebe and Gaddy's work. These 100°C data are not consistent with subsequent and apparently more accurate data from Coan and King (1971) (Figure 6), and were not included in Appendix A. The H_2O solubilities from Todheide and Frank (1963) at 50 and 100°C (Figure 6) fall above the trend defined by other data. However, these authors acknowledge a significant error margin ($\pm$ 1 mole percent) in their results. The H_2O solubilities of Müller et al. (1988) at 100°C fall fairly well in line with those of Coan and King (1971) (Figure 6).

The large departure from ideal behavior at pressures above approximately 20 bar results from the fact that H_2O molecules become quite "uncomfortable" (Prausnitz et al., 1986) as they become surrounded by much more abundant CO_2 molecules at low temperatures and high pressures. As discussed previously, the sharp discontinuity in H_2O solubility at subcritical temperatures (Figure 4) coincides with the phase change from a gaseous to a liquid CO_2-rich phase. The pressure interval over which three phases coexist (H_2O-rich liquid, CO_2-rich gas, and CO_2-rich liquid) is very small (Figures 2 and 3) and, using only the solubility data, is difficult to distinguish from the saturation pressure of pure CO_2 at any given temperature (see Wenland et al., 1999, for measurements on the three-phase coexistence line). Above this saturation pressure (or more precisely above this three-phase pressure interval), the H_2O solubility in the CO_2-rich phase increases with pressure

and temperature (e.g., from roughly 0.3 and 0.4 mole percent between 100 and 400 bar at 25°C, and from 0.8 to 1.4 mole percent over the same pressure range at 75°C). Above the critical temperature, the H_2O solubility trend with pressure becomes progressively smoother, as would be expected.

CO_2 Solubility in the H_2O-Rich Phase

With respect to CO_2 solubility in water, there is good agreement between the data of King et al. (1992) at 20°C and those of Rosenbauer et al. (2001) at 21°C (Figure 4) and between those of King et al. (1992) and Wiebe and Gaddy (1940) at 25°C (Figure 5). Solubilities reported more recently by Teng et al. (1997) at 15 and 20ºC are fairly consistent with those of King et al. (1992), but are up to 5% higher than those reported by King et al. above 200 bar (Figure 4). Solubilities from Todheide and Frank (1963) and Wiebe and Gaddy (1939) at 50°C and 100°C plot on the same trends (Figures 6). The same is true for the data of Müller et al. (1988) and those of Wiebe and Gaddy (1939) at 100ºC. The rest of the reviewed data falls closely on these trends, with the exception of the CO_2 solubilities measured by Gillepsie and Wilson (1982) at 15°C (Figure 4) and of Sako et al. (1991) at 75°C (Figure 6) (which deviate by up to 15% or so from the other data).

The CO_2 solubility in water increases sharply with pressure up to the three-phase pressure interval (nearly undistinguishable from the saturation pressure of pure CO_2, as mentioned previously and shown on Figures 2 and 3) and less so after this point (Figures 4 to 6). Below the critical temperature, the CO_2 solubility trend with pressure reflects two solubility curves for two distinct phases: liquid CO_2 above saturation pressures, and gaseous CO_2 below these pressures. This results in a sharp break in slope on each of the overall solubility trends at subcritical temperatures. Above the critical temperature, the CO_2 solubility trend reflects only one solubility curve for gaseous CO_2 with a bend in the vicinity of the critical point that smoothly diminishes away from this point (Figures 5 and 6). At the critical point, the solubilities of liquid and gaseous CO_2 solubilities in water should be equal.

The effect of temperature on CO_2 solubility is less pronounced than that of pressure, with solubility decreasing as temperature increases. The decrease with temperature is less noticeable at high pressure than at lower pressure (e.g., the solubility decreases from approximately 3 to 2.6 mole percent between 25 and 100°C at 400 bar, but from approximately 2.5 to 1.4 mole percent between the same temperatures at 100 bar; Figures 5 and 6).

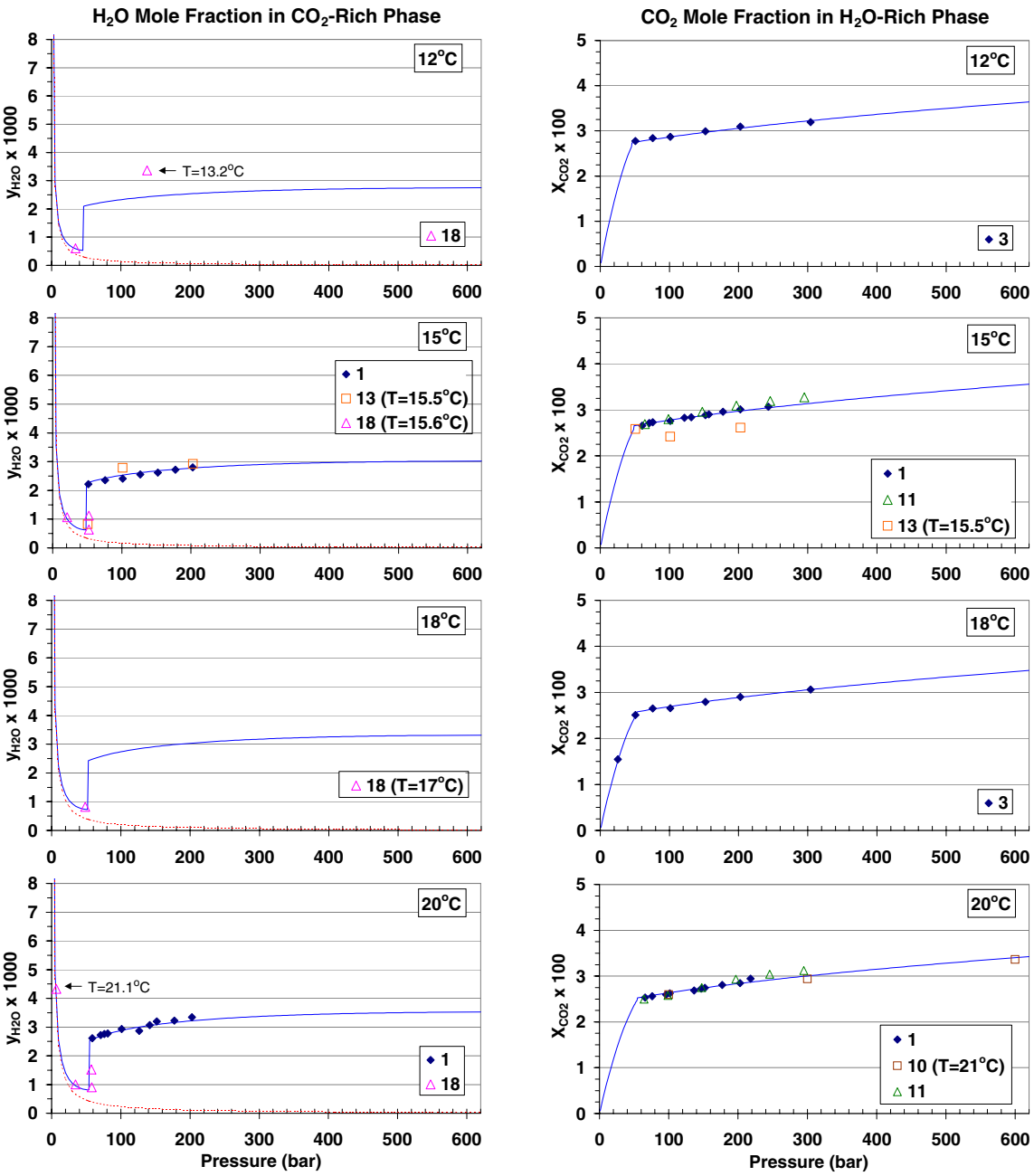

Figure 4. Mutual solubilities of H_2O and CO_2 at 12, 15, 18, and 20 ºC and pressures to 600 bar. Experimental data (Appendix A) are shown as symbols, with sources given below. Solubilities computed using Equations 21–28 and parameters in Tables 1 and 2 are shown as solid lines (References 11 and 13–18 were not used in calculating these lines.) The dashed lines are calculated assuming ideal mixing. See text. Reference numbers are as follows: (1) King et al. (1992), (2) Wiebe and Gaddy (1941), (3) Wiebe and Gaddy (1940), (4) Wiebe and Gaddy (1939), (5) Coan and King (1971), (6) Todheide and Frank (1963), (7) Takenouchi and Kennedy (1961), (8) Jackson et al. (1995), (9) Greenwood and Barnes (1966), (10) Rosenbauer et al. (2001), (11) Teng et al. (1997), (12) Müller et al. (1988), (13) Gillepsie and Wilson (1982), (14) Briones et al. (1987), (15) D'Souza et al. (1988), (16) Sako et al. (1991), (17) Dohrn et al. (1993), and (18) Song and Kobayashi (1987).

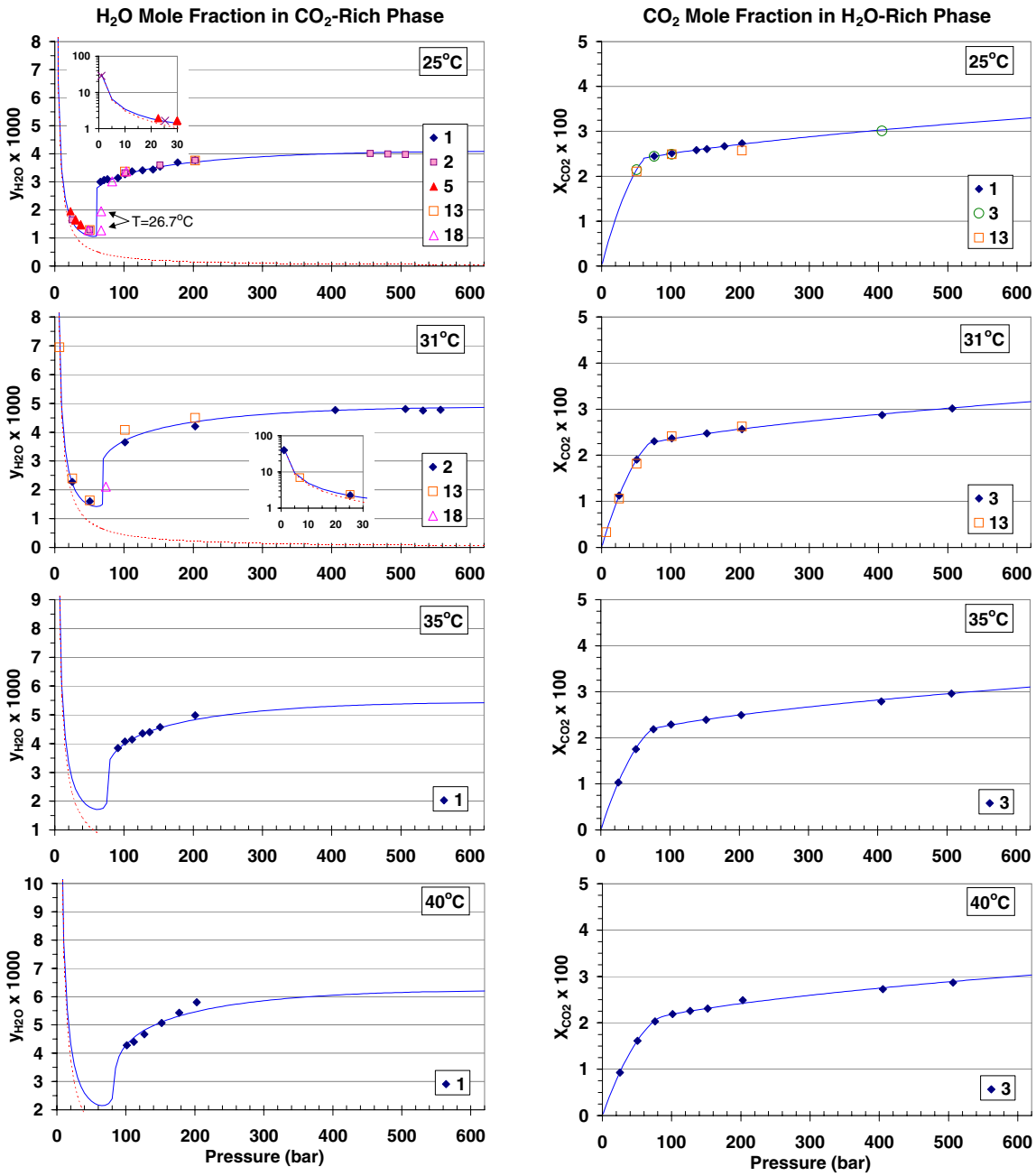

Figure 5. Mutual solubilities of H_2O and CO_2 at 25, 31.04, 35, and 40 ºC and pressures to 600 bar. Experimental data (Appendix A) are shown as symbols (see caption of Figure 1 for data sources). Solubilities computed using Equations 21–28 and parameters in Tables 1 and 2 are shown as solid lines (References 11 and 13–18 were not used in calculating these lines.) The dashed lines are calculated assuming ideal mixing. See text.

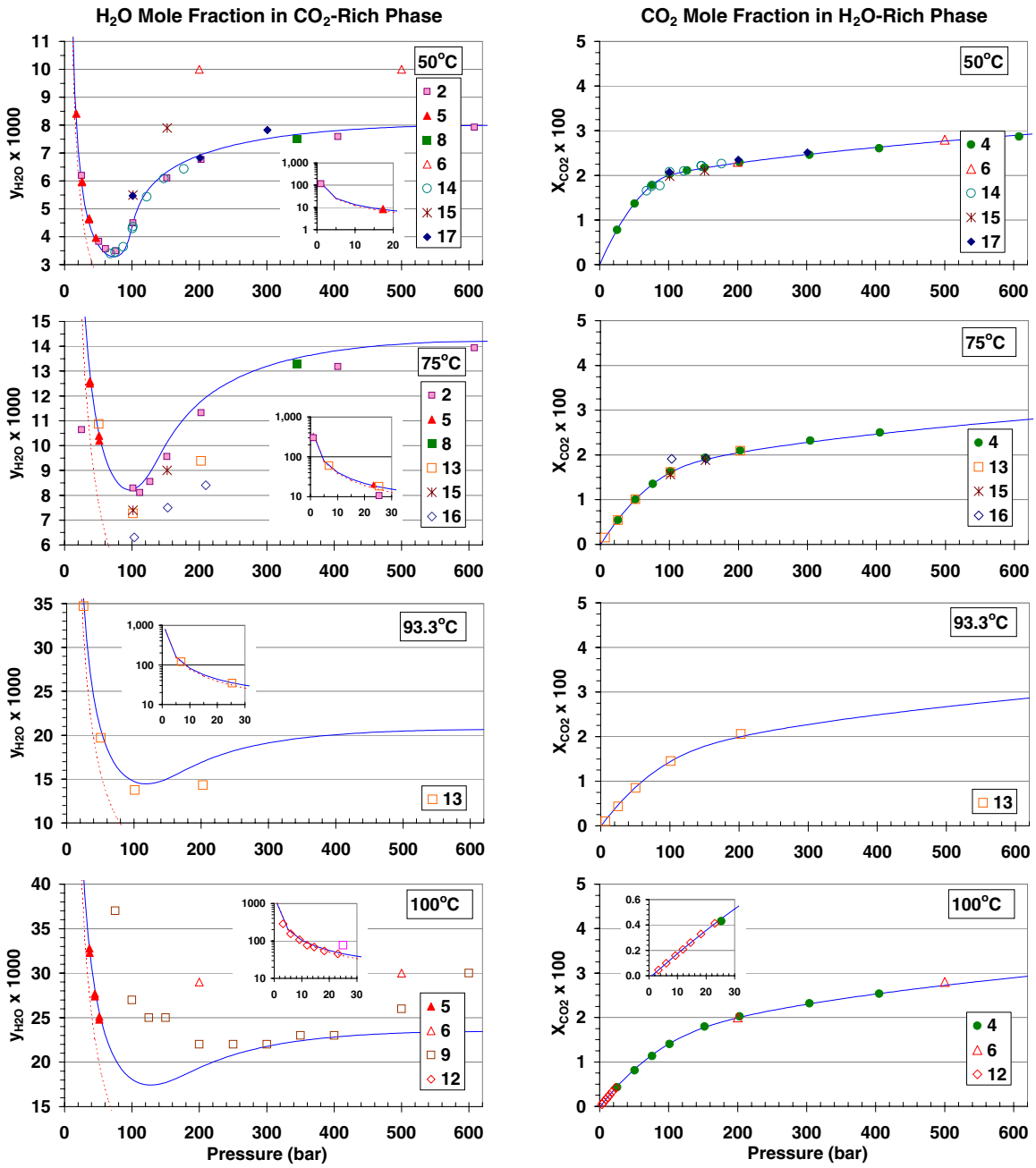

Figure 6. Mutual solubilities of H_2O and CO_2 at 50, 75, 93.3, and 100 ºC and pressures to 600 bar. Experimental data (Appendix A) are shown as symbols (see caption of Figure 1 for data sources). Solubilities computed using Equations 21–28 and parameters in Tables 1 and 2 are shown as solid lines (References 11 and 13–18 were not used in calculating these lines.) The dashed lines are calculated assuming ideal mixing. See text.

Calculation of Mutual H_2O and CO_2 Solubilities

Thermodynamic Formulation

The compositions of two-phase gas-liquid mixtures at various pressures and temperatures can be calculated by equating the chemical potentials of species in the liquid (μ_i^l) and gas (μ_i^g) phases, which is the condition required for equilibrium (e.g., Denbigh, 1983). In this case, we write:

$$\mu_i^l = \mu_i^g \quad (1)$$

with

$$\mu_i^l = \mu^{0\,l}_i + RT \ln(f_i^l/f^{0\,l}_i) \quad (2)$$

$$\mu_i^g = \mu^{0\,g}_i + RT \ln(f_i^g/f^{0\,g}_i) \quad (3)$$

where subscript *i* refers to each species at equilibrium, *g* and *l* refer to gas and liquid phases, respectively, f are the fugacities of each species, and μ^0 and f^0 are the chemical potentials and fugacities at a given reference standard state. If the standard state is chosen to be the same for both the liquid and gas phases (generally $f^0_i = 1$ bar), then Equation (1) simplifies to equating the fugacities f_i^l and f_i^g. Methods for calculating the mutual solubilities of liquids and compressed gases by equating fugacities are thoroughly described in Prausnitz et al. (1986), and have been used either directly or indirectly by various authors to express P-T-X properties of two-phase H_2O-CO_2 mixtures (e.g., Coan and King, 1971; Spycher and Reed, 1988; King et al., 1992). Similar procedures using somewhat different conventions for standard states and activities have been used by Crovetto (1991), Carroll and Mather (1992), and Müller et al. (1988) to calculate the solubility of CO_2 in water.

Here, we use a similar approach except that we recast the equality of chemical potentials (Equation 1) through "true" equilibrium constants for the reactions between the liquid and gas phases, where the reference standard states and activities are consistent with

those typically used in geochemical studies (e.g., Helgeson and Kirkham, 1974; Helgeson et al., 1981). The approach also can be easily extended to take into account any nonideality of the liquid phase (e.g., due to addition of salts) as well as gas-phase nonideality.

At equilibrium, the following reactions and corresponding equilibrium constants can be written:

$$H_2O(l) \text{ <==> } H_2O(g) \qquad K_{H2O} = f_{H2O(g)} / a_{H2O(l)} \tag{4}$$

$$CO_2(aq) \text{ <==> } CO_2(g) \qquad K_{CO2(g)} = f_{CO2(g)} / a_{CO2(aq)} \tag{5}$$

where f are fugacities of the gas components and a are activities of components in the liquid (aqueous) phase (here by definition equal to f^1/f^0_1). In this case, the pure water standard state is chosen as unit activity at all pressures and temperatures. For dissolved species like aqueous CO_2, the standard state is chosen as unit activity in a hypothetical 1 molal solution at infinite dilution. A pressure correction needs to be applied to the equilibrium constants at pressures deviating significantly from the reference pressure. The correction can be approximated by the "Poynting" factor (e.g. Prausnitz et al., 1986) such that

$$K_{(T,P)} = K^0_{(T,P^o)} \exp\left(\frac{(P - P^0)\,\overline{V}_i}{R\,T} \right) \tag{6}$$

where $\overline{V}_i$ is the average partial molar volume of the pure condensed component *i* over the pressure interval P^0 to P, where P^0 is the reference pressure (in this case 1 bar). Equation (6) derives directly from the fundamental relationship $(\partial\mu/\partial P)_T = V$. Equation (6) yields a correction typically less than 10% below 100 bar, but becomes significantly larger at higher pressures. As discussed later, values of K^0_{H2O}, K^0_{CO2}, $\overline{V}_{H2O}$ and $\overline{V}_{CO2}$ can be taken directly from the literature and/or fitted to experimental solubility data.

If CO_2 changes from a gaseous to a liquid state as pressure increases (at subcritical temperatures), additional free energy terms related to the phase transition need to be added to Equation (6). An alternative to adding extra terms in Equation (6), however, is to consider another equilibrium constant in this equation, $K^0_{CO2(l)}$, referring to liquid instead of gaseous CO_2. This equilibrium constant is then used in place of $K^0_{CO2(g)}$ when the temperature is subcritical and the pressure is above the CO_2 saturation pressure, with the values of $K^0_{CO2(l)}$ and $K^0_{CO2(g)}$ being equal at the critical temperature. This is the approach adopted in this study. Also, the dissociation of $CO_{2(aq)}$ to bicarbonate (HCO_3^-) can be safely ignored because the pK for this reaction at the temperatures considered here ranges between approximately 6.0 and 6.6, whereas the solution pH at the CO_2 pressures considered is less than 4.

From the definition of fugacity and partial pressures (e.g., Prausnitz et al., 1986; Hala et al. 1967, Denbigh 1983), we then write

$$f_i = \Phi_i P_i \tag{7}$$

$$P_i = y_i P_{tot} \tag{8}$$

and thus

$$f_i = \Phi_i y_i P_{tot} \tag{9}$$

where Φ_i, y_i, and P_i are the fugacity coefficient, mole fraction, and partial pressure of component *i* in the gas phase, respectively, and P_{tot} is the total pressure (note: hereafter, y always denotes mole fraction in the CO_2-rich phase, whereas x is used for mole fraction in the aqueous phase). Substituting Equation (9) in (4) and (5) then yields:

$$f_{H2O} = \Phi_{H2O}\, y_{H2O}\, P_{tot} = K_{H2O}\, a_{H2O(l)} \tag{10}$$

$$f_{CO2} = \Phi_{CO2}\, y_{CO2}\, P_{tot} = K_{CO2(g)}\, a_{CO2(aq)} \tag{11}$$

Recasting Equation (10) to express the water mole fraction in the gas phase and applying the pressure correction to K_{H2O} from Equation (6) yields:

$$y_{H2O} = \frac{K^0_{H2O}\, a_{H2O}}{\Phi_{H2O}\, P_{tot}} \exp\left(\frac{(P - P^0)\,\overline{V}_{H2O}}{R\,T}\right) \tag{12}$$

A fairly good approximation (within 10% in our considered P-T range) of water mole fractions in the CO_2-rich phase can be computed with this equation if a_{H2O} is assumed to be unity. However, for better accuracy at high pressures, the water activity deviation from unity caused by dissolved CO_2 should be taken into account. At the pressures and temperatures considered here, the CO_2 solubility is sufficiently small such that Raoult's law can be used to set the water activity (a_{H2O}) equal to its mole fraction in the water phase (x_{H2O}). For a system where H_2O and CO_2 are the only two components, x_{H2O} is directly calculated as $1\text{-}x_{CO2}$ such that:

$$y_{H2O} = \frac{K^0_{H2O}\,(1 - x_{CO2})}{\Phi_{H2O}\, P_{tot}} \exp\left(\frac{(P - P^0)\,\overline{V}_{H2O}}{R\,T}\right) \tag{13}$$

The mole fraction of aqueous CO_2 (x_{CO2}) is then computed from its molality m (i.e. moles/kg_{H2O}, such that $x_{CO2} = m_{CO2}/(m_{CO2} + 55.508)$ with CO_2 and H_2O being the only components). The molality is derived directly from Equation (11) by setting

$$a_{CO2} = \gamma\, m_{CO2} \tag{14}$$

where γ is the activity coefficient of dissolved CO_2. For this electrically neutral species, if no salts are present, the activity coefficient for the reference state and convention used here is set to $\gamma = 1/(1 + m_{CO2}/55.508)$, which is a molality to mole fraction correction (e.g., Denbigh, 1983; Helgeson et al., 1981) yielding a unit activity coefficient on the mole fraction scale. Further correction for nonideality is not considered at this stage because the solubility of CO_2 in water is small. Substituted in Equation (14), this relationship yields

$$x_{CO2} = a_{CO2} / 55.508 \tag{15}$$

which, with substitution of Equations (5) and (6) for a_{CO2}, and Equation (11) for f_{CO2} gives

$$x_{CO2} = \frac{\Phi_{CO2} (1 - y_{H2O}) P_{tot}}{55.508 K^0_{CO2(g)}} \exp\left(- \frac{(P - P^0) \overline{V}_{CO2}}{R T} \right) \tag{16}$$

Equations (13) and (16) have essentially the same form as those derived by assuming equality of fugacities in the gas and aqueous phase (e.g., Prausnitz, 1986; King et al., 1992), except that the gas fugacities are expressed through the use of true equilibrium constants and the activities of liquid H_2O and aqueous CO_2.

The fugacity coefficients in Equations (13) and (16) must be derived from the P-V-T properties of H_2O and CO_2 mixtures, preferably using an equation of state. The Redlich-Kwong equation, and variations of it, have been used successfully to represent the properties of H_2O-CO_2 mixtures over various P-T ranges (e.g., de Santis et al., 1974; Kerrick and Jacobs, 1981; King et al. 1992). This equation of state has the advantage of representing properties of gases and their mixtures fairly well over extended P-T ranges and in the vicinity of the critical point. Also, for gas mixtures, mixing rules for parameters in this equation yield relatively simple expressions. The disadvantage of the Redlich-Kwong equation is that it is a cubic equation in volume that is somewhat cumbersome to use. Virial equations of state in terms of only pressure and temperature have the advantage of being more easily implemented in numerical models where pressure and temperature are primary variables (e.g., Spycher and Reed, 1988). However, the treatment of gas mixtures with virial-type expressions is more tedious than with the Redlich-Kwong equation, especially for expansions after the second virial coefficient. For any practical applications to gas mixtures, the treatment generally should be limited to two virial coefficients, but this limit seriously degrades accuracy in the vicinity of, and below, the critical point. For example, such treatment with the equations of Spycher and Reed (1988) for H_2O-CO_2 mixtures provides fairly good approximations

for CO_2 down to approximately 50°C at 500 bar (the CO_2 is nearly pure in this case), but breaks down for H_2O in the gas mixture above approximately 150 bar at 50°C. In contrast, using the Redlich-Kwong equation, King et al. (1992) were able to represent within a few percent their P-T-X data and those of Wiebe and Gaddy (1940 and 1941) from 15 to 40°C and up to 500 bar. For these reasons, we decided to adopt the Redlich-Kwong equation, rather than a virial treatment, to compute the fugacity coefficients necessary to solve Equations (13) and (16).

The Redlich-Kwong equation takes the form (e.g., Prausnitz et al., 1986):

$$Z = \frac{P\,V}{R\,T} = \left(\frac{V}{V - b}\right) - \left(\frac{a}{R\,T^{1.5}\,(V + b)}\right) \tag{17}$$

or

$$P = \left(\frac{R\,T}{V - b}\right) - \left(\frac{a}{T^{0.5}\,V\,(V + b)}\right) \tag{18}$$

where parameter a and b represent measures of attractive molecular forces and molecular size, respectively. Z is the compressibility factor, V the volume of the gas phase, and R the gas constant. For mixtures, parameters a and b can be calculated by the following mixing rules (e.g., Prausnitz et al., 1986):

$$a_{mix} = \sum_{i=1}^{n}\sum_{j=1}^{n} y_i y_j a_{ij} \tag{19}$$

$$b_{mix} = \sum_{i=1}^{n} y_i b_i \tag{20}$$

where a_{mix} and b_{mix} replace a and b in Equation (17) or (18). For the binary H_2O-CO_2 mixture, therefore:

$$a_{mix} = y_{H2O}^2\, a_{H2O} + 2\, y_{H2O}\, y_{CO2}\, a_{H2O\text{-}CO2} + y_{CO2}^2\, a_{CO2} \tag{21}$$

$$b_{mix} = y_{H2O}\, b_{H2O} + y_{CO2}\, b_{CO2} \tag{22}$$

Based on these mixing rules and Equation (17) or (18) it can be shown, through the relationship $\ln(\Phi) = \int \frac{(Z-1)}{P} dP$, that the fugacity coefficient, Φ_k, of component *k* in mixtures with other components *i* is given by (e.g., Prausnitz et al., 1986):

$$\ln(\Phi_k) = \ln\left(\frac{V}{V - b_{mix}}\right) + \left(\frac{b_k}{V - b_{mix}}\right) - \left(\frac{2\sum_{i=1}^{n} y_i a_{ik}}{R\,T^{1.5}\,b_{mix}}\right) \ln\left(\frac{V + b_{mix}}{V}\right) + \left(\frac{a_{mix}\,b_k}{R\,T^{1.5}\,b_{mix}^2}\right)\left[\ln\left(\frac{V+b}{V}\right) - \left(\frac{b_{mix}}{V + b_{mix}}\right)\right] - \ln\left(\frac{P\,V}{R\,T}\right) \quad (23)$$

It is apparent from this equation that the fugacity coefficient of each component in the gas mixture depends on the mixture composition (in addition to pressure and temperature). Therefore, Equation (23) (and 17 or 18 to calculate P, V, or T from two of these three variables) needs to be solved simultaneously with Equations (13) and (16) to compute the mutual solubilities of CO_2 and H_2O. This requires an iterative scheme that could add significant burden for implementation into already computationally intensive fluid flow/transport models. However, King et al. (1992) have shown that at low temperatures (15 to 40ºC), for all practical purposes, infinite H_2O dilution can be assumed in the CO_2-rich phase when using Equations (17) to (23). That is, the assumption is made that $y_{H2O} = 0$ and $y_{CO2} = 1$ in the mixing rules applied to the equation of state. By doing so, the fugacity coefficients Φ_{H2O} and Φ_{CO2} can be computed in a direct, noniterative, manner. The fugacity coefficient of CO_2 (nearly pure) in the mixture is approximated as that of pure CO_2, while the strongly nonideal mixing behavior is still captured by the calculation of the H_2O fugacity coefficient in the gas mixture. Here, the same approach is adopted and shown to provide adequate results up to at least 75°C.

Numerical Implementation

Fugacity coefficients of CO_2 and H_2O in the gas mixture are calculated first (provided that Redlich-Kwong parameters have been determined as reported further below). To do so, the volume (V) of the mixture is calculated from input values of pressure and

temperature using Equation (17) or (18). This also yields the compressibility factor Z for the gas mixture. We set y_{CO2}=1 and y_{H2O}=0 in the mixing rules (Equations 21 and 22), which equates to using the Redlich-Kwong paremeters a and b for pure CO_2. Thus, Equation 18 is solved independently from Equations (13) and (16).

The volume is computed by recasting Equation (18) as a general cubic equation in terms of volume,

$$V^3 - V^2\left(\frac{R\,T}{P}\right) - V\left(\frac{R\,T\,b}{P} - \frac{a}{P\,T^{0.5}} + b^2\right) - \left(\frac{a\,b}{P\,T^{0.5}}\right) = 0 \qquad (24)$$

then solving this equation directly using the method of Nickalls (1993). Below the critical point, this equation can yield more than one volume value as it attempts to reproduce the liquid-gas phase transition (Figure 7). The volume value to use depends on which phase, liquid or gas, is stable at a given pressure and temperature. The volume of the gas phase, V_{gas}, is always given by the maximum root of Equation 24 (Figure 7). The minimum root always provides the volume of the liquid phase, V_{liquid}. The phase transition occurs at the point where the work w_1 done from V_{gas} to V_{liquid} along a straight path is the same as the work w_2 done along the curved path depicted by Equation 18 (Figure 7) (e.g., Adamson, 1979). From the work definition ($w = \int P\,dV$) w_1 is easily computed as

$$w_1 = P\,(V_{gas} - V_{liquid}) \qquad (25)$$

and w_2 is given by differentiating Equation 18 between V_{gas} and V_{liquid} to obtain

$$w_2 = R\,T \ln\left(\frac{V_{gas} - b}{V_{liquid} - b}\right) + \frac{a}{T^{0.5}\,b} \ln\left(\frac{(V_{gas} + b)\,V_{liquid}}{(V_{liquid} + b)\,V_{gas}}\right) \qquad (26)$$

For any pressure and temperature, the volume of the stable phase is then computed according to the following criteria: if (w2 – w1) > 0, then V is taken as the maximum root of Equation 18, and if (w2 – w1) < 0, then V is taken as the minimum root. If (w2 – w1) = 0, two phases are stable and, therefore, both roots provide a correct answer.

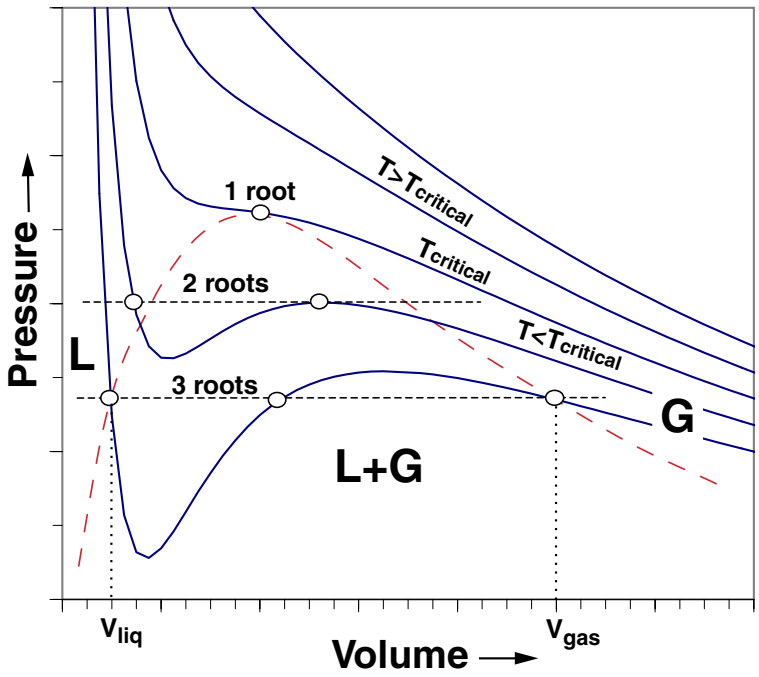

Figure 7. Illustration of P-V-T relationships calculated with the Redlich-Kwong equation (Equation 24) or similar equations of state for a pure fluid (G=gas, L=liquid, and the dashed line denotes the phase boundary). Given pressure and temperature as inputs, more than one volume value (root) are computed below the critical point. See text.

Once the volume of the CO_2-rich phase is computed, it is substituted directly into Equation (23) to compute fugacity coefficients. Again, we set $y_{CO2}=1$ and $y_{H2O}=0$ in this equation and the mixing rules, so that Φ_{H2O} and Φ_{CO2} can be computed independently of each other and of Equations (13), (16), and (18). Using the fugacity coefficients computed in this way, Equations (13) and (16) are solved directly by setting:

$$A = \frac{K^0_{H2O}}{\Phi_{H2O}\, P_{tot}} \exp\left(\frac{(P - P^0)\,\overline{V}_{H2O}}{R\,T}\right) \tag{27}$$

$$B = \frac{\Phi_{CO2}\, P_{tot}}{55.508\, K^0_{CO2(g)}} \exp\left(-\frac{(P - P^0)\,\overline{V}_{CO2}}{R\,T}\right) \tag{28}$$

such that

$$y_{H2O} = \frac{(1 - B)}{(1/A - B)} \tag{29}$$

Equation (29) provides the water solubility in the CO_2-rich phase. This equation simplifies to $y_{H2O} = A$ if the term B is neglected (which corresponds to the assumption of unit water activity, as discussed earlier for Equation 12). Knowing y_{H2O}, the aqueous CO_2 mole fraction is then given by

$$x_{CO2} = B\,(1 - y_{H2O}) \tag{30}$$

Because y_{H2O} is typically small (Figures 4 to 6), fairly good approximations of x_{CO2} (within an error equal to y_{H2O}) can be computed by setting $x_{CO2} = B$. In our case, however, the full forms of Equations (29) and (30) are used.

As mentioned earlier, at subcritical temperatures and pressures above saturation values, $K^0_{CO2(g)}$ in Equation (28) needs to be replaced with another equilibrium constant, $K^0_{CO2(l)}$, referring to liquid instead of gaseous CO_2. The method implemented here uses $K^0_{CO2(l)}$ in place of $K^0_{CO2(g)}$ when both the following conditions are met: (1) temperature is below 31°C (near the critical temperature of pure CO_2) and (2) the calculated volume using Equation (24) is less than 94 cm^3/mol (near the critical volume of pure CO_2). Because of the infinite dilution assumption, the calculated phase-change boundary for the CO_2-rich phase is the same as for pure CO_2, and the P-T space in which three phases coexist (CO_2 gas, CO_2 liquid, and H_2O liquid) is ignored. This approximation can be justified on the basis that the three-phase P-T space is quite small and, in fact, essentially indiscernable using the available experimental solubility data (Figures 2 and 3). It should be also recognized that the Redlich Kwong equation is too simple to accurately reproduce the phase transition boundary in P-V-T space (Figure 7) and thus yields only an approximation of the P-T saturation curve. In this respect, volumes calculated with Equation (24) can be used to distinguish between liquid and gaseous phases away from the saturation curve (by a few bars in our case) but not closer. However, as shown later,

the calculated volume values have a sufficient accuracy to reproduce the fugacities of both liquid and gaseous CO_2 generally within one percent of published reference data.

Determination of Redlich-Kwong Parameters and Equilibrium Constants

The procedure described above to compute mutual solubilities was implemented into a computer routine. Parameters needed for implementation of this method were obtained from the literature, where available, and by calibration (fitting procedure) to the data in Appendix A and to other published reference data as discussed below. Model calibration was performed automatically using the PEST-ASP v5.0 freeware, a powerful model-independent nonlinear parameter estimation package (Doherty, 2002).

King et al. (1992) determined values of a_{CO2} and b_{CO2} (for Equations 17–23) by fitting the Redlich-Kwong equation to volumetric and fugacity data computed using the equation of state of Huang et al. (1985) for pure CO_2. These authors then fitted equations similar to those discussed above (expressed in terms of Henry's law constants and equality of fugacities) to their experimental data (from 15 to 40°C and up to 200 bar), to obtain values of b_{H2O} and $a_{H2O\text{-}CO2}$, as well as CO_2 solubilities (Henry's law constants) and average partial molar volume $\overline{V}_{CO2}$. However, using their data, we could not reproduce accurately the mutual solubilities of H_2O and CO_2 over our broader temperature and pressure range. Therefore, a refit of available data was necessary, as discussed below. In doing so, solubilities could be reproduced generally within a few percent of experimental values over a temperature range from 12°C to 110°C for x_{CO2} and from 15 to 100°C for y_{H2O}, to pressures of 600 bar.

Fugacity coefficient values for pure CO_2 given in the International Union of Pure and Applied Chemistry (IUPAC) tables (Angus et al., 1976) were fitted to Equations (18)–(23) from 280 to 380 K (6.85 to 106.85°C) and from 1 to 600 bar to yield values of a_{CO2} and b_{CO2} (the 6.85°C temperature was below our targeted temperature range of 12°C, but the closest isotherm given below 16.85°C in the IUPAC tables). The value of b_{CO2} was fitted as a constant, because this term represents a molecular size that should not vary with temperature or pressure. To obtain good fits, we had to vary the value of a_{CO2}

(intermolecular attraction) with temperature. This parameter is not a smooth function of temperature (e.g., deSantis et al., 1974). However, within the limited temperature range considered here, good results could be obtained by using a simple linear dependency of this parameter with temperature (Table 1). In doing so, fugacity coefficients were reproduced mostly within 0.5% of the IUPAC values, with a mean absolute error of 0.2% (Figure 8). It is important to keep in mind, however, that an accurate fit of fugacities does not necessarily translate to similarly accurate calculations of P-V-T properties, as discussed below. Values of a_{CO2} and b_{CO2} determined in this way are fairly close, but slightly higher, than those reported by King et al. (1992) (which range between 6.27 and 6.20 x 10^7 bar cm^6 $K^{0.5}$ mol^{-2} for a_{CO2} and 27.2 to 27.3 cm^3/mol for b_{CO2} from 15 to 40°C).

Table 1. Redlich-Kwong parameters for Equations (17)–(24). Values of b_{H2O} and $a_{H2O\text{-}CO2}$ were derived assuming infinite dilution of H_2O in the compressed gas phase (i.e. $y_{H2O} = 0$ and $y_{CO2} = 1$ in these equations; a value for a_{H2O} is not needed). See text.

Parameter	Value		Units
a_{CO2}	$7.54 \times 10^7 - 4.02 \times 10^4 \times T_{(in\ °K)}$ (fitted T range: 280-380ºK)		bar cm^6 $K^{0.5}$ mol^{-2}
	T (°C)	a_{CO2}	
	15	6.38×10^7	
	25	6.34×10^7	
	50	6.24×10^7	
	75	6.14×10^7	
	100	6.04×10^7	
b_{CO2}	27.86		cm^3/mol
b_{H2O}	18.10		cm^3/mol
$a_{H2O\text{-}CO2}$	7.89×10^7		bar cm^6 $K^{0.5}$ mol^{-2}

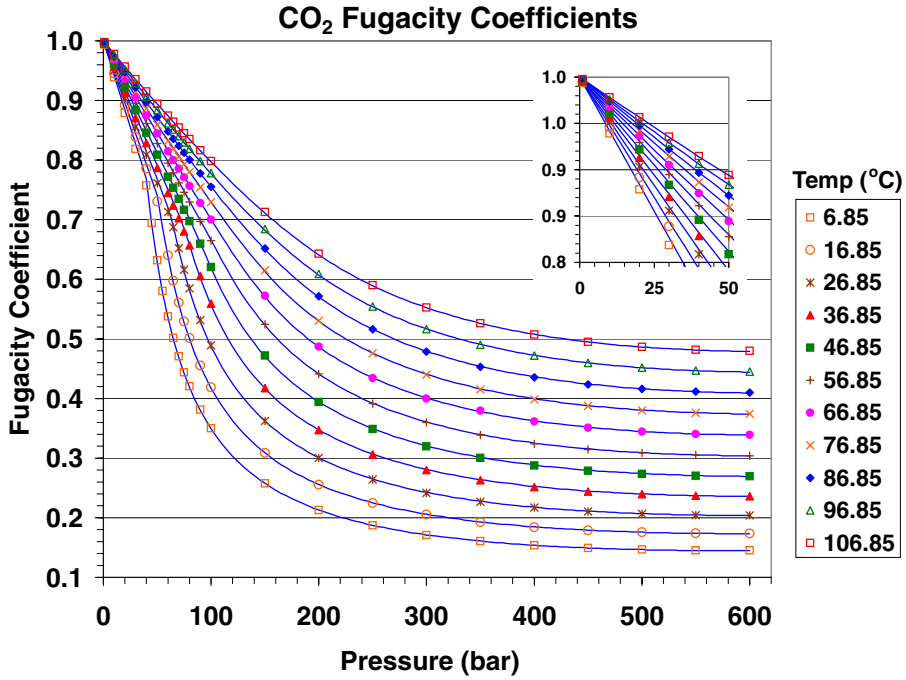

Figure 8. Fugacity coefficient of pure CO_2 between 6.85 and 106.85°C (290-380°K) up to 600 bar. Reference data (symbols) are from Angus et al. (1976). Values computed using Equations 21–24 and parameters in Table 1 are shown as solid lines. See text.

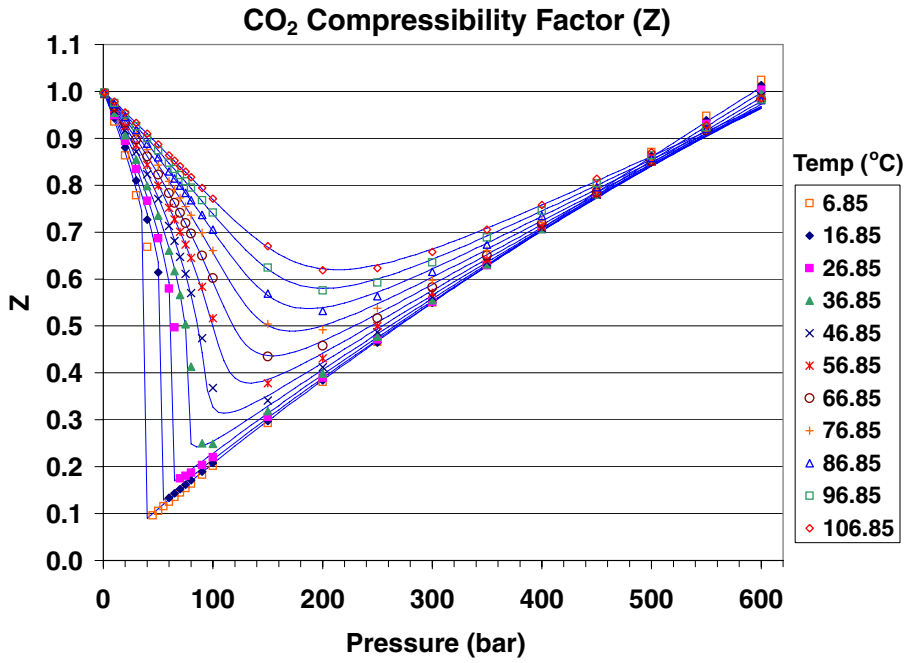

Figure 9. Compressibility factor of pure CO_2 between 6.85 and 106.85°C (290-380°K) up to 600 bar. Reference data (symbols) are from Angus et al. (1976). Values computed using Equation 24 and parameters in Table 1 are shown as solid lines. See text.

Compressibility factors computed using the values of a_{CO2} and b_{CO2} in Table 1, determined from the fugacity coefficient data, are generally within 5% of the IUPAC values, with a mean absolute error of 1.4% when ignoring the 6.85°C isotherm (Figure 9). Within a few bar from the phase boundary (along the steep portion of the curves on Figure 9), errors can be much higher depending on whether a gaseous phase or liquid phase volume is computed. As a result, the Redlich-Kwong equation and parameters in Table 1 cannot accurately reproduce the P-T saturation curve of CO_2, yielding saturation pressures off by approximately 2 bar at 12°C to 5 bar at 31°C when compared to the data of Span and Wagner (1996). In any case, the critical parameters needed to calculate solubilities are the fugacity coefficients, which are reproduced quite well by the Redlich-Kwong equation and parameters in Table 1.

Once values of a_{CO2} and b_{CO2} were determined, values of $a_{H2O\text{-}CO2}$ and b_{H2O} were obtained by inverting simultaneously most of the mutual solubility data given in Appendix A. Points above approximately 600 bar and 100°C (beyond our range of interest and outside the range of the fit of the CO_2 fugacity coefficients) and clear outliers were either ignored or given much lower weights than other points. The data of Teng et al. (1997) were not included in the inversion because their trend differed somewhat from the trend defined by the data of King et al. (1992) and Rosenbauer et al. (2001) (Figure 4). The data of Gillepsie and Wilson (1982), Briones et al. (1987), D'Souza et al. (1988), Sako et al. (1991), Dohrn et al. (1993), and Song and Kobayashi (1987) were not used either because they were acquired at a later stage of this study. However, as discussed later, these data (References 11 and 13–18 on Figures 4–6) were used to evaluate the accuracy of predicted solubilities in the P-T ranges where no measurements were fitted.

To determine the parameters $a_{H2O\text{-}CO2}$ and b_{H2O} through inversion of the solubility data, values of K^0_{H2O}, $K^0_{CO2(g)}$, $K^0_{CO2(l)}$, $\overline{V}_{H2O}$ and $\overline{V}_{CO2}$ for Equations (27) and (28) were also necessary. A value of a_{H2O} was not needed because of the infinite H_2O dilution assumption. One possible approach was to determine all these parameters simultaneously in one fit. However, to limit the initial degrees of freedom of such inversion, and for consistency with available thermodynamic data for H_2O and CO_2, we first attempted to fit

only $a_{H2O\text{-}CO2}$ and b_{H2O}, and use values for the other parameters from the literature as described below.

Because of the choice of standard state (unit activity of water at all temperatures and pressures), values of K^0_{H2O} are given directly by the fugacity values of pure H_2O at saturation pressures reported by Helgeson and Kirkham (1974). These values were regressed as a polynomial function of temperature (Table 2). An average partial molar volume value ($\overline{V}_{H2O}$) of 18.5 cm^3/mol was estimated from the volume data in Helgeson and Kirkham (1974), and yielded satisfactory results that could not be significantly improved by further adjusting this parameter. For this reason, we did not attempt to fit this parameter, nor K^0_{H2O}.

Initial values of $K^0_{CO2(g)}$ consistent with the standard state and activity coefficient convention used here were computed using SUPCRT92 (Johnson et al. 1992). These calculations made use of the HKF equation of state for aqueous species and parameters given in Shock et al. (1989), and thermodynamic properties from Wagman et al. (1982) and Kelley (1960) for $CO_{2(aq)}$ and $CO_{2(g)}$. Values of $K^0_{CO2(g)}$ calculated with SUPCRT92 are in relatively good agreement with the Henry's law constants values (converted to true equilibrium constants) calculated by other authors (Table 2). However, when comparing these values, it must be kept in mind that some of these values relate to systems in which CO_2 is in the liquid state (King et al., 1992), whereas others reflect gaseous CO_2 data (Crovetto, 1991, and values calculated with SUPCRT92).

A first inversion of the solubility database was done using the $K^0_{CO2(g)}$ and $\overline{V}_{CO2}$ values from SUPCRT92 (Table 2) to estimate $a_{H2O\text{-}CO2}$ and b_{H2O}, without distinguishing the solubilities of gaseous and liquid CO_2. In doing so, an approximate fit of the CO_2 solubility data was obtained, yielding deviations up to 10% at temperatures below 20°C and above 75°C. A second inversion of the mutual H_2O and CO_2 solubility data set was then performed including $K^0_{CO2(g)}$ (expressed as a polynomial function of temperature) and $\overline{V}_{CO2}$ as unknown parameters in addition to $a_{H2O\text{-}CO2}$ and b_{H2O}, but still without

Table 2. Equilibrium constants and average partial molar volumes for Equations (27) and (28), and regression parameters for $\log(K^0)_{T,1\ bar} = a + bT + cT^2 + dT^3 + eT^4$ with temperature in °C. The meaning of K is defined by Equations (4)–(6).

Species	$\log(K^0)_{T,1bar}$ 15	25	31	40	50	75	100	$\overline{V}_i$ (cm^3/mol)	Reference
H_2O	-1.768	-1.499	-1.347	-1.132	-0.910	-0.418	-0.002	18.5	Helgeson and Kirkham (1974)
$CO_{2(g)}$	1.372	1.481	1.541	1.624	1.705	1.862	1.951	32.1	This Study (see text)
	-	-	-	-	1.703	1.860	1.951	28.6-35.1	Carroll and Mather (1992)[b]
	-	-	-	-	-	-	1.954	-	Müller et al. (1988)[b]
	1.347	1.472	1.539	1.628	1.713	1.875	1.981	-	Crovetto (1991)[b]
	1.339	1.469	1.537	1.627	1.712	1.871	1.969	33.8[a]	SUPCRT92 (see text)
$CO_{2(l)}$	1.361[c]	1.476[c]	1.541[c]	-	-	-	-	32.1	This Study (see text)
$CO_{2(l),/(g)}$	1.347[c]	1.474[c]	-	1.628	-	-	-	32.0	King et al. (1992)[b]

Species	Regression coefficients a	b	c	d	e
H_2O	-2.215 (fitted T range: 0-150ºC)	3.162×10^{-2}	-1.294×10^{-4}	4.187×10^{-7}	-7.331×10^{-10}
$CO_{2\ (g)}$	1.188 (fitted T range: 12-110ºC)	1.307×10^{-2}	-5.445×10^{-5}	0.0	0.0
$CO_{2\ (l)}$	1.168 (fitted T range: 12-31ºC)	1.361×10^{-2}	-5.135×10^{-5}	0.0	0.0

[a] Average of values computed with SUPCRT92 between 15 and 100°C and from 1 to 500 bar

[b] Converted from Henry's law constants K_H using Equation (15) for activities [$\log(K) = \log(55.508/K_H)$]

[c] At these temperatures, the fitted solubility data reflect a liquid CO_2-rich phase

distinguishing between the solubilities of liquid and gaseous CO_2. Finally, a third inversion of the mutual solubility data set was performed to simultaneously estimate $K^0_{CO2(g)}$, $K^0_{CO2(l)}$ (as two separate polynomial functions of temperature), $\overline{V}_{CO2}$, $a_{H2O\text{-}CO2}$, and b_{H2O}. Initial-guess values for each successive inversions were provided by the results of the previous inversion. No significant fit improvement was obtained by expressing $\overline{V}_{CO2}$ or $a_{H2O\text{-}CO2}$ as simple functions of temperature. Values of parameters fitted in this

way are shown in Tables 1 and 2. The fitted $K^0_{CO2(g)}$, $K^0_{CO2(l)}$, and $\overline{V}_{CO2}$ values are within the range of values from other studies (Table 2) and further discussed later. The $a_{H2O\text{-}CO2}$ and b_{H2O} values are slightly higher than those reported by King et al. (1992) (who report $a_{H2O\text{-}CO2} = 7.67 \times 10^7$ bar cm^6 $K^{0.5}$ mol^{-2} and $b_{H2O} = 16.6$ cm^3/mol). It should be noted that the values of parameters b_{H2O} and $a_{H2O\text{-}CO2}$ in Table 1 reflect the assumption of infinite dilution of H_2O in the compressed gas phase and should not be used in mixing models that do not make this assumption.

Using the parameters determined from this final inversion (Tables 1 and 2) and Equations (21) through (30) (with $y_{H2O} = 0$ and $y_{CO2} = 1$ in Equations 21-23), fitted experimental H_2O solubilities were reproduced with a mean absolute error around 4% (2% for points above 75 bar) and individual errors less than 5% for the majority of the data points. The fitted experimental CO_2 solubilities were reproduced with a mean absolute error around 1% and the majority of individual errors less than 1%.

Discussion and Conclusions

Calculated mutual solubilities using Equations (21)–(30) and parameters in Tables 1 and 2 are shown as solid lines on Figures 4 to 6. Ideal solubilities of H_2O in the compressed gas phase (calculated as $y_{H2O} = P^0_{saturation\ H2O} / P_{total}$) are also shown on these figures and clearly indicate that the assumption of ideal mixing for water in the CO_2-rich phase could lead to large discrepancies.

It was mentioned above that the trend of CO_2 solubility with pressure at given subcritical temperatures reflects two distinct solubility curves, one for liquid CO_2 and the other for gaseous CO_2. These two solubility curves should cross exactly at the phase transition point. However, because the Redlich Kwong equation cannot precisely predict the location of the phase change in P-T space, the model does not switch from the gas to the liquid solubility curve exactly where it should (in this case, the liquid solubility curve extends slightly into metastable space). This does not affect the shape of each individual solubility curve (gas or liquid), nor does it affect the fit of the experimental data. It only results in a minute jump in the computed CO_2 solubility at the phase transition point,

noticeable only on subcritical isotherms computed using small pressure increments (< 1 bar) across the phase boundary.

From 12°C up to 50°C, agreement between calculated and experimental solubilities is quite good and generally within a few percent up to pressures near 600 bar. Points not included in the fit of solubility data (labeled with reference numbers 11 and 13–8 in Figures 4,5, and 6) were also closely reproduced (true predictions in these cases), with exceptions falling clearly off the trend of the majority of the data. For example, predicted H_2O solubilities at low temperatures in the vicinity of the CO_2 gas-liquid phase boundary line up well with solubilities reported by Song and Kobayashi (1987), even though the data reported by these authors were not used in the model calibration (Figure 4).

At 75 and 100°C and pressures above 50 bar, the available H_2O solubility data become scattered (Figure 6) and the accuracy of the model is more difficult to evaluate. The 93°C data of Gillepsie et al. (1987) are reproduced within 5% up to 100 bar, even though their measured solubilities were not used in deriving the model parameters (Figure 6). At 200 bar, however, the calculated H_2O solubility is higher by approximately 20% than the value reported by these authors. The 100°C data include points from Greenwood and Barnes (1966) that were not included in the data inversion (nor in Appendix A) because they appear to have been extrapolated from the work of Wiebe and Gaddy (1941). The only other H_2O solubility data at 100°C and pressure above 100 bar are those reported by Todheide and Frank (1963), which were reported with a low precision around $\pm$1 mole percent. To further evaluate the model accuracy in this general temperature range, we also considered solubilities reported at 110°C by Takenouchi and Kennedy (1964) (Figure 10). The H_2O solubilities reported by these authors follow a more defined trend than the 100°C data. However, this trend clearly cannot be reproduced by the calculations (Figure 10). As the H_2O mole fraction in the compressed gas phase increases with temperature, the assumption of infinite H_2O dilution eventually breaks down. Therefore, calculated H_2O solubilities are expected to become progressively less accurate as temperature increases. This could be a reason for the poor H_2O solubility fit at 110°C. However, we also attempted to reproduce the H_2O solubility in the 75–110°C

range without assuming infinite dilution. This required a fully iterative treatment of Equations (23)–(30) and a value for a_{H2O}, for which we tested values from various sources, including values fitted together with the other Redlich-Kwong parameters. In doing so, the experimental data still could not be reproduced much better than shown here. This suggests there could be problems with the higher-temperature data in addition to the calculation limitations.

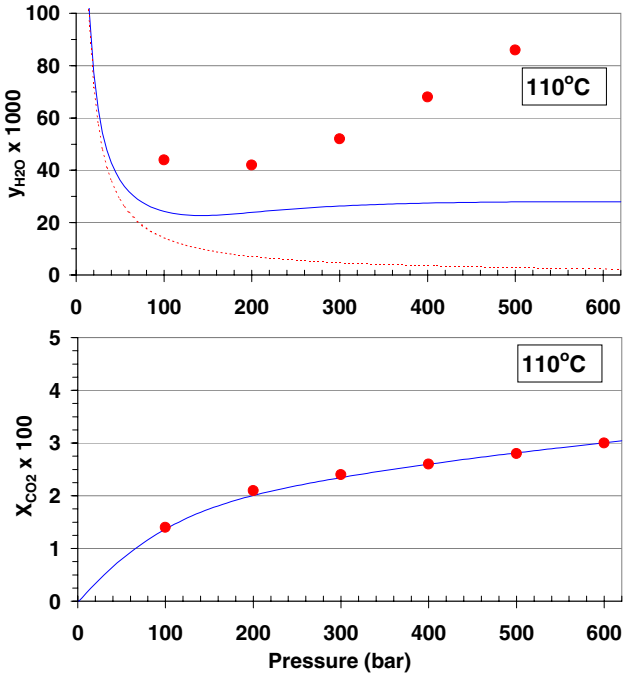

Figure 10. Mutual solubilities of H_2O and CO_2 at 110ºC and pressures to 600 bar. Experimental data from Takenouchi and Kennedy (1964) (Appendix A) are shown as symbols. Solubilities computed using Equations 21–28 and parameters in Tables 1 and 2 are shown as solid lines. The dashed lines are calculated assuming ideal mixing. See text.

Because the mutual solubilities of CO_2 and H_2O were fitted simultaneously, the CO_2 log(K) values determined in this way reflect actual data for both the CO_2- and H_2O-rich phases. However, these solubility constants reflect the use of an average CO_2 partial molar volume fitted over the entire temperature range of interest. In addition, the fitted equilibrium constants reflect the assumptions made regarding the activities of water and $CO_{2(aq)}$ and other uncertainties associated with the parameters necessary to compute fugacities. Therefore, these constants should be used only with other parameters given in Tables 1 and 2.

No claims are made that the CO_2 solubility constants fitted in this study are more, or less, accurate than other values shown in Table 2. Our log(K) value at 100ºC matches closely the values derived from Henry's law constants reported by both Müller et al. (1988) and Carroll and Mather (1992). However, each data source has its own share of assumptions and potential problems. Crovetto (1991) used a more comprehensive set of aqueous solubility data, but had to calculate water mole fractions in the gas phase (rather than rely on measured data) to compute her values of Henry's law constants. This author also omitted data in our P-T range of interest (specifically, points above 2 bar and between 0 and 80 ºC) because of difficulties in evaluating data near the critical point. Carroll and Mather (1992) used measured gas-phase compositions to derive Henry's law constants, but did not cover data below 50ºC. Log(K) values derived from their reported Henry's law constants between 50 and 100ºC are in close agreement with our estimated log(K) values (Table 2). However, these authors fitted each isotherm separately, and obtained inconsistent trends of partial molal volume variation with temperature, and a value possibly too low at 100ºC (28.6 cm^3/mol) (e.g., Garcia, 2001). These authors also had to exclude the data of Müller et al. (1988) in their analyses to obtain physical values of volume at 100ºC. This may be partly caused by the fact that for each isotherm, these authors attempted to fit an activity model for $CO_{2(aq)}$ (a Margules parameter) in addition to the partial molal volume and the Henry's law constant. This could have resulted in "overfitting" the data because the activity of $CO_{2(aq)}$ is likely to remain very close to unity at the small concentrations considered. Also note that the log(K) values derived from the Henry's law constants reported by King et al. (1992) and Crovetto (1991) at 15ºC are identical. However, the study of King et al. involved liquid CO_2 below the critical temperature, whereas Crovetto (1991) considered only experimental studies in which gaseous CO_2 was present. Therefore, it is fortuitous that some of the log(K) values in Table 2 match exactly. The general agreement between the various solubility constant values would seem to indicate that aqueous solubility differences caused by the CO_2 phase change in the 12–31ºC temperature range are small and apparently within the range of errors introduced by the various correlation approaches and experimental procedures.

The method presented here to compute the mutual solubilities of H_2O and CO_2 is essentially a reformulation of the standard approach of equating fugacities to calculate P-T-X properties of phases at equilibrium. The formulation relies on basic thermodynamic principles and could be easily extended to saline solutions through the use of published activity models for water and aqueous species. Simplifications resulting from the assumption of infinite dilution of H_2O in the CO_2-rich phase improves computing efficiency because an iterative solution scheme is not required. This assumption was originally shown by King et al. (1992) to work well at temperatures up to 40°C for the H_2O-CO_2 system. Our study suggests that this approximation can be made to temperatures of at least 75°C and possibly 100°C. It should be noted again, however, that the equation of state and calculation methods applied here do not yield volumetric data that would be accurate enough to derive precise thermodynamic properties of the compressed gas mixture or to derive precise liquid-gas phase boundaries. The approach was intended for efficient calculation of mutual solubilities in numerical models used to study the feasibility of CO_2 geologic sequestration. It will also be useful for other practical applications involving geochemical systems at temperatures between 12 and 100°C and pressures up to 600 bar.

Acknowledgment

The authors wish to acknowledge John Apps, George Moridis, Sonia Salah, and Julio Garcia for their review and constructive comments for improvement of this paper. This work was supported by the US Department of Energy through the Office of Basic Energy Sciences under Contract No. DE-AC03-76SF00098. One author (JEK) wishes to acknowledge support from the Australian Petroleum Cooperative Research Center's GEODISC project.

References

Adamson A.W., 1979. A Textbook of Physical Chemistry. 2nd. Ed. Academic Press, New York, 123 p.

Anderson, G. K., 2002. Solubility of carbon dioxide in water under incipient clathrate formation conditions. J. Chem. Eng. Data, 47, 219–222.

Angus, S., Armstrong, B. and De Reuck, K.M., 1976. International Thermodynamic Tables of the Fluid State. 3. Carbon dioxide. Int. Union of Pure and Applied Chemistry. Pergamon Press, 385 p.

Briones, J.A., Mullins, J.C., Thies, M.C., 1987. Ternary phase equilibria for acetic acid-water mixtures with supercritical carbon dioxide. Fuild Phase Equilib., 36, 235–246.

Carroll, J.J and Mather, A.E., 1992. The system carbon dioxide-water and the Krichevsky-Kasarnovsky equation. J. of Solution Chemistry, 21, 607–621.

Coan, C.R. and King, Jr., A.D., 1971. Solubility of water in compressed carbon dioxide, nitrous oxide, and ethane. Evidence for hydration of carbon dioxide and nitrous oxide in the gas phase. J. Am. Chem. Soc., 93, 1857–1862.

Crovetto, R., 1991. Evaluation of solubility data for the system CO_2-H_2O from 273 K to the critical point of water. J. Phys. Chem. Ref. Data, 20, 575–589.

Dohrn, R., Bünz, Devlieghere, F., and Thelen D., 1993. Experimental measurements of phase equilibria for ternary and quaternary systems of glucose, water, CO_2 and ethanol with a novel apparatus. Fluid Phase Equilib., 83, 149–158.

Denbigh, K., 1983. The Principles of Chemical Equilibrium, 4th. ed., Cambridge Univ. Press, 494 p.

DeSantis, R., Breedveld, G.J.F., and Prausnitz, J. M., 1974. Thermodynamic properties of aqueous gas mixtures at advanced pressures. Ind. Chem. Process Design Develop. 13, No. 4, 374–377.

DOE, 1999. Carbon sequestration research and development. Report DOE/SC/FE-1, U.S. Department of Energy, Office of Science, Office of Fossil Energy, Washington, D.C.

Doherty, J., 2002. PEST - Model-independent parameter estimation. Watermark Numerical Computing, Corinda 4075, Brisbane, Australia.

D'Souza, R., Patrick, J.R., and Teja, A.S., 1988. High pressure phase equilibria in the carbon dioxide - n-hexadecane and carbon dioxide-water systems. Can. J. Chem. Eng., 66, 319–323.

Evelein, K.A., Moore, R.G., and Heidemann, R.A., 1976. Correlation of the phase behavior in the systems hydrogen sulfide-water and carbon dioxide-water. Ind. Eng. Chem. Proc. Des. Dev.,15, No.3, 423–428.

Fan, S-S. and Guo, T-M., 1999. Hydrate formation of CO_2-rich binary and quaternary gas mixtures in aqueous sodium chloride solutions. J. Chem. Eng. Data, 44, No.4, 829–832.

Garcia, J.E., 2001. Density of aqueous solutions of CO_2. LBNL Report 49023. Lawrence Berkeley National Laboratory, Berkeley, California.

Gillepsie, P.C. and Wilson, G.M., 1982. Vapor-liquid and liquid-liquid equilibria: water-methane, water-carbon dioxide, water-hydrogen sulfide, water-npentane, water-methane-npentane. Research report RR-48, Gas Processors Association, Tulsa Okla., April 1982.

Greenwood, H.J. and Barnes, H.L., 1966. Binary mixtures of volatile components. In Section 17, Handbook of Physical Constants, Clark S.P. (ed). The Geological Society of America Memoir 97.

Hala, E., Pick, J., Fried, V. and Vilim, O., 1967. Vapor-Liquid Equilibrium. (English trans. by G. Standart). Pergamon Press, 599 p.

Helgeson, H.C., Kirkham, D.H., 1974. Theoretical prediction of the thermodynamic behavior of aqueous electrolytes at high pressures and temperatures: I. Summary of the thermodynamic/electrostatic properties of the solvent. Am. J. Sci., 274, 1089,1198.

Helgeson, H.C., Kirkham, D.H., Flowers G.C., 1981. Theoretical prediction of the thermodynamic behavior of aqueous electrolytes at high pressures and temperatures: IV. Calculation of activity coefficients, osmotic coefficients, and apparent molal and standard and relative partial molal properties to 600°C and 5 kb. American Journal of Science, 281: 1249–1516.

Huang, F.H., Li, M.H., Lee, L.L., Starling, K.E., and Chung, F.T.H., 1985. An accurate equation of state for carbon dioxide. J. Chem. Eng. Japan, 18, 490.

Jackson, K., Bowman, L.E., Fulton, J.L., 1995. Water solubility measurements in supercritical fluids and high-pressure liquids using near-infrared spectroscopy. Anal. Chem., 67, 2368–2372.

Johnson, J.W., Oelkers, E., and Helgeson, H.C., 1992. SUPCRT92: A software package for calculating the standard molal thermodynamic properties of minerals, gases, aqueous species and reactions from 1 to 5000 bar and 0 to 1000°C. Comput. Geosci., 18, 899–947.

Kelley, K.K., 1960. Contributions to the Data in Theoretical Metallurgy XIII: High Temperature Heat Content, Heat Capacities and Entropy Data for the Elements and

Inorganic Compounds. U.S. Bureau of Mines Bulletin 584, 232 p.

Kennedy, G.C. and Holser, W.T., 1966. Pressure-volume-temperature and phase relations of water and carbon dioxide. In Section 16, Handbook of Physical Constants, Clark S.P. (ed). The Geological Society of America Memoir 97.

Kerrick, D.M. and Jacobs, G.K., 1981. A modified Redlich-Kwong equation for H2O, CO_2 and H_2O-CO_2 mixtures at elevated pressures and temperatures. Am. J. Sci., 281, 735–767.

King, M.B., Mubarak, A., Kim, J.D. and Bott, T.R., 1992. The mutual solubilities of water with supercritical and liquid carbon dioxide. J. Supercrit. Fluids, 5, 296–302.

Mäder, U.K., 1991. H_2O-CO_2 mixtures: a review of P-V-T-X data and an assessment from a phase equilibrium point of view. Can. Mineral., 29, 767–790.

Müller, G., Bender, E., and Maurer, G., 1988. Das Dampf-Flüssigkeitsgleichgewicht des ternären Systems Ammoniak-Kohlendioxid-Wasser bei hohen Wassergehalten im Bereich zwischen 373 und 473 Kelvin. Berichte der Bunsen-Gesellshaft für Physikalische Chemie, 92, 148–160.

Ng, H-J. and Robinson, D.B., 1985. Hydrate formation in systems containing methane, ethane, propane, carbon dioxide or hydrogren sulfide in the presence of methanol. Fluid Phase Equilib., 21, 145–155.

Nickalls, R.W.D., 1993. A new approach to solving the cubic: Cardan's solution revealed. The Mathematical Gazette, 77, 354–359.

Prausnitz, J.M., Lichtenthaller, R.N., and De Azedevo, E.G., 1986. Molecular thermodynamics of fluid phase equilibria. Prentice Hall, 353p.

Pruess, K., and Garcia, J., 2002. Multiphase flow dynamics during CO_2 disposal into saline aquifers. Environ. Geol., 42, 282–295.

Rosenbauer, R. J., Bischoff, J. L., and Koksalan, T., 2001. An Experimental Approach to CO_2 Sequestration in Saline Aquifers: Application to Paradox Valley, CO. Eos Trans. AGU, 82(47), Fall Meet. Suppl., Abstract V32B-0974, 2001.

Sako, T., Sugeta, T., Nakazawa, N., Obuko, T., Sato, M., Taguchi, T., and Hiaki, T., 1991. Phase equilibrium study of extraction and concentration of furfural produced in reactor using supercritical carbon dioxide. Jour. Chem. Engineering Japan, 24, 449–454.

Shock, E.L., Helgeson, H.C., and Sverjensky, D.A., 1989. Calculation of the thermodynamic and transport properties of aqueous species at high pressures and temperatures: Standard partial molal properties of inorganic neutral species: Geochim. Cosmochim. Acta, 53, p. 2157–2183.

Spycher, N.F. and Reed, M.H., 1988. Fugacity coefficients of H_2, CO_2, CH_4, H_2O and H_2O-CO_2-CH_4 mixtures: a virial equation treatment for moderate pressures and temperatures applicable to hydrothermal boiling. Geochim. Cosmochim. Acta, 52, 739–749.

Song, K.Y. and Kobayashi, R., 1987. Water content of CO_2 in equilibrium with liquid water and/or hydrates. SPE Formation Evaluation, 2, 500–508 (Society of Petroleum Engineers).

Span, R. and Wagner, W., 1996. A new equation of state for carbon dioxide covering the fluid region from the triple-point temperature to 1100K at pressures up to 800 MPa. J. Phys. Chem. Ref. Data, 25, No.6, 1509–1596.

Takenouchi, S. and Kennedy, G.C., 1964. The binary system H_2O-CO_2 at high temperatures and pressures. Am. J. Sci., 262, 1055–1074.

Teng, H., Yamasaki, A., Chun, M.-K., and Lee, H., 1997. Solubility of liquid CO_2 in water at temperatures from 278 K to 293 K and pressures from 6.44 MPa to 29.49 MPa and densities of the corresponding aqueous solutions. J. Chem. Thermodyn., 29, 1301–1310.

Tödheide, K. and Frank, E.U., 1963. Das Zweiphasengebiet und die kritische Kurve im System Kohlendioxid-Wasser bis zu Drucken von 3500 bar. Z. Phys. Chemie, Neue Folge 37, 387–401.

Wagman, D.D., Evans, W.H., Parker, V.B., Schumm, R.H., Halow, I., Bailey, S.M., Churney, K.L., Nuttall, R.L., 1982, The NBS Tables of Chemical and Thermodynamic Properties: J. Phys. Chem. Ref. Data, V. 11, supplement No. 2, 392 p.

Wendland, M., Hasse, H., and Maurer, G., 1999. Experimental pressure-temperature data on three- and four-phase equilibria of fluid, hydrate, and ice phases in the system carbon dioxide-water. J. Chem. Eng. Data, 44, No.5, 901–906.

Wiebe, R. and Gaddy, V.L., 1939. The solubility in water of carbon dioxide at 50, 75, and 100°, at pressures to 700 atmospheres. J. Am. Chem. Soc. 61, 315–318.

Wiebe, R. and Gaddy, V.L., 1940. The solubility of carbon dioxide in water at various temperatures from 12 to 40° and at pressures to 500 atmospheres: critical phenomena. J. Am. Chem. Soc. 62, 815–817.

Wiebe, R. and Gaddy, V.L., 1941. Vapor phase composition of carbon dioxide-water mixtures at various temperatures and at pressures to 700 atmospheres. J. Am. Chem. Soc. 63, 475–477.

Appendix A

Mutual Solubilities of CO_2 and H_2O
Reviewed Experimental Data from 12 to 110°C and from 1 to 700 bar

T (C)	P (bar)	y H2O (‰)	x CO2 (%)	ref. gas	ref. liq.
12	34.5	0.6030		18	
12	50.7		2.777		3
12	76.0		2.837		3
12	101.3		2.871		3
12	152.0		2.993		3
12	202.7		3.098		3
12	304.0		3.196		3
13.17	137.9	3.3627		18	
13.78	82.8	2.7852		18	
15	51.7	2.22		1	
15	60.8		2.658		1
15	64.4		2.69		11
15	70.9		2.716		1
15	76.0	2.35	2.729	1	1
15	98.7		2.80		11
15	101.3	2.41	2.757	1	1
15	121.6		2.828		1
15	126.7	2.55		1	
15	131.7		2.84		1
15	147.7		2.96		11
15	152.0	2.62	2.886	1	1
15	157.1		2.902		1
15	177.3	2.72	2.960	1	1
15	196.8		3.09		11
15	202.7	2.80	3.013	1	1
15	243.2		3.07		1
15	245.8		3.19		11
15	294.9		3.27		11
15.56	20.7	1.0656		18	18
15.56	52.4	0.6400 (g)		18	
15.56	52.4	1.1200 (l)		18	
15.6	50.7	0.819	2.58	13	13
15.6	101.4	2.78	2.42	13	13
15.6	202.7	2.92	2.61	13	13
17	48.3	0.8229		18	
18	25.3		1.544		3
18	50.7		2.510		3
18	76.0		2.649		3
18	101.3		2.659		3
18	152.0		2.793		3

T (C)	P (bar)	y H2O (‰)	x CO2 (%)	ref. gas	ref. liq.
18	202.7		2.901		3
18	304.0		3.063		3
20	34.5	1.0010		18	
20	58.8	2.61		1	
20	64.4		2.50		11
20	65.9		2.531		1
20	70.9	2.72		1	
20	76.0	2.76	2.563	1	1
20	81.1	2.78		1	
20	96.3		2.597		1
20	98.7		2.58		11
20	101.3	2.93	2.625	1	1
20	126.7	2.87		1	
20	136.8		2.689		1
20	141.9	3.07		1	
20	146.9		2.727		1
20	147.7		2.75		11
20	152.0	3.20	2.743	1	1
20	177.3	3.22	2.807	1	1
20	196.8		2.93		11
20	202.7	3.34	2.847	1	1
20	217.9		2.945		1
20	245.8		3.04		11
20	294.9		3.12		11
20.2	57.9	0.8999 (g)		18	
20.2	57.9	1.5000 (l)		18	
21	100		2.59		10
21	300		2.94		10
21	600		3.36		10
21.1	6.9	4.3276		18	
25	1.0	28.62		2	
25	22.7	1.95		5	
25	25.3	1.64		2	
25	29.8	1.63		5	
25	30.0	1.67		5	
25	37.3	1.45		5	
25	37.4	1.49		5	
25	48.3	1.2787		18	
25	50.7	1.28	2.10	13	13
25	50.7	1.29	2.142	2	3
25	65.9	3.00		1	
25	70.9	3.07		1	
25	76.0		2.444		3
25	76.0	3.09	2.445	1	1

T (C)	P (bar)	y H2O (‰)	x CO2 (%)	ref. gas	ref. liq.
25	82.8	3.0152		18	
25	91.2	3.14		1	
25	101.3	3.27	2.510	1	1
25	101.3	3.32	2.488	2	3
25	101.4	3.36	2.49	13	13
25	103.4	3.3739		18	
25	111.5	3.37		1	
25	126.7	3.41		1	
25	136.8		2.582		1
25	141.9	3.44		1	
25	152.0	3.54	2.603	1	1
25	152.0	3.60		2	
25	177.3	3.69	2.672	1	1
25	202.7	3.76	2.57	13	13
25	202.7	3.78	2.734	1	1
25	202.7	3.77		2	
25	405.3		3.011		3
25	456.0	4.01		2	
25	481.3	3.99		2	
25	506.6	3.97		2	
26.67	66.9	1.2700 (g)		18	
26.67	66.9	1.9541 (l)		18	
29.4	55.2	1.57	2.03	13	13
29.4	101.4	3.89	2.39	13	13
29.4	202.7	4.36	2.63	13	13
29.5	71.7	1.4981 (g)		18	
29.5	71.7	2.1940 (l)		18	
31.04	1.0	39.8		2	
31.04	25.3	2.28	1.127	2	3
31.04	50.7	1.61	1.904	2	3
31.04	76.0		2.303		3
31.04	101.3	3.65	2.368	2	3
31.04	152.0		2.476		3
31.04	202.7	4.21	2.567	2	3
31.04	405.3	4.77	2.871	2	3
31.04	506.6	4.80	3.014	2	3
31.04	532.0	4.75		2	
31.04	557.3	4.78		2	
31.05	6.9	6.94	0.331	13	13
31.05	25.3	2.39	1.056	13	13
31.05	50.7	1.63	1.817	13	13
31.05	101.4	4.08	2.41	13	13
31.05	202.7	4.50	2.62	13	13

T (C)	P (bar)	y H2O (‰)	x CO2 (%)	ref. gas	ref. liq.
31.06	73.9	2.1079		18	
35	25.3		1.030		3
35	50.7		1.754		3
35	76.0		2.189		3
35	91.2	3.84		1	
35	101.3	4.07	2.288	1	3
35	111.5	4.14		1	
35	126.7	4.35		1	
35	136.8	4.40		1	
35	152.0	4.57	2.394	1	3
35	202.7	4.98	2.495	1	3
35	405.3		2.792		3
35	506.6		2.963		3
40	25.3		0.925		3
40	50.7		1.609		3
40	76.0		2.032		3
40	101.3	4.28	2.186	1	3
40	111.5	4.40		1	
40	126.7	4.67	2.256	1	3
40	152.0	5.07	2.308	1	3
40	177.3	5.43		1	
40	202.7	5.80	2.488	1	3
40	405.3		2.726		3
40	506.6		2.868		3
50	1.0	115.71		2	
50	17.3	8.41		5	
50	25.3	6.20	0.774	2	4
50	25.5	5.95		5	
50	25.8	5.98		5	
50	36.4	4.66		5	
50	36.4	4.63		5	
50	46.3	3.96		5	
50	50.7	3.83	1.367	2	4
50	60.8	3.57		2	
50	68.2	3.39	1.651	14	14
50	75.3	3.45	1.750	14	14
50	76.0	3.50	1.779	2	4
50	87.2	3.64	1.768	14	14
50	100.6	4.29		14	
50	101	5.47	2.075	17	17
50	101.3	4.36	2.081	14	14
50	101.3	4.49	2.018	2	4
50	101.33	5.5	1.98	15	15
50	122.1	5.43	2.096	14	14
50	126.7		2.106		4
50	147.5	6.08	2.215	14	14
50	147.5		2.207		14

T (C)	P (bar)	y H2O (‰)	x CO2 (%)	ref. gas	ref. liq.
50	152.0	6.10	2.174	2	4
50	152	7.9	2.10	15	15
50	176.8	6.43	2.262	14	14
50	200.0	10	2.3	6	6
50	201	6.82	2.347	17	17
50	202.7	6.77	2.289	2	4
50	301	7.82	2.514	17	17
50	304.0		2.457		4
50	344.8	7.50		8	
50	405.3	7.59	2.606	2	4
50	500.0	10	2.8	6	6
50	608.0	7.93	2.868	2	4
50	709.3	8.01	2.989	2	4
75	1.0	301.09		2	
75	6.9	60.14	0.149	13	13
75	25.3	18.16	0.542	13	13
75	25.3	10.64	0.545	2	4
75	23.3	20.00		5	
75	37.4	12.50		5	
75	37.5	12.60		5	
75	50.7	10.87	1.006	13	13
75	50.7		1.002		4
75	51.3	10.40		5	
75	51.5	10.20		5	
75	76.0		1.351		4
75	101.3	8.29	1.630	2	4
75	101.33	7.4	1.56	15	15
75	101.4	7.27	1.616	13	13
75	103.4	6.3	1.91	16	16
75	111.5	8.11		2	
75	126.7	8.55		2	
75	152.0	9.56	1.937	2	4
75	152.00	9.0	1.88	15	15
75	153.1	7.5	1.92	16	16
75	202.7	9.38	2.09	13	13
75	202.7	11.32	2.098	2	4
75	209.4	8.4		16	
75	304.0		2.317		4
75	344.8	13.30		8	
75	405.3	13.19	2.498	2	4
75	608.0	13.93		2	
75	709.3	14.00	2.933	2	4
93.3	6.9	120.3	0.0973	13	13
93.3	25.3	34.71	0.435	13	13
93.3	50.7	19.70	0.846	13	13
93.3	101.4	13.74	1.45	13	13
93.3	202.7	14.32	2.06	13	13

T (C)	P (bar)	y H2O (‰)	x CO2 (%)	ref. gas	ref. liq.
100	3.25	288	0.045	12	12
100	6	155	0.098	12	12
100	9.2	107	0.159	12	12
100	11.91	77	0.208	12	12
100	14.52	69	0.261	12	12
100	18.16	54	0.328	12	12
100	23.07	45	0.414	12	12
100	25.3		0.429		4
100	36.8	32.80		5	
100	37.2	32.30		5	
100	44.8	27.70		5	
100	44.8	27.40		5	
100	50.7		0.812		4
100	51.5	24.80		5	
100	51.5	25.10		5	
100	76.0		1.135		4
100	101.3		1.400		4
100	152.0		1.794		4
100	200.0	29.00	2.0	6	6
100	202.7		2.023		4
100	304.0		2.318		4
100	405.3		2.537		4
100	500.0	30.00	2.8	6	6
100	709.3		3.002		4
110	100	44	1.4	7	7
110	200	42	2.1	7	7
110	300	52	2.4	7	7
110	500	86	2.8	7	7
110	600	107	3	7	7
110	700	128	3.15	7	7

Notes: (g) and (l) refer to H_2O solubilities reported in coexisting gaseous and liquid CO_2, respectively.

References:

1 King et al. (1992)
2 Wiebe and Gaddy (1941)
3 Wiebe and Gaddy (1940)
4 Wiebe and Gaddy (1939)
5 Coan and King (1971)
6 Todheide and Frank (1963)
7 Takenouchi and Kennedy (1961)
8 Jackson et al. (1995)
(9 Not used)
10 Rosenbauer et al. (2001)
11 Teng et al. (1997)
12 Müller et al. (1988)
13 Gillepsie and Wilson (1982)
14 Briones et al. (1987)
15 D'Souza et al. (1988)
16 Sako et al. (1991)
17 Dohrn et al. (1993)
18 Song and Kobayashi (1987)